Session II: Beams and shear walls

Session II

Beams and Shear Walls

Leere Seite
Blank page
Page vide

Plastic Analysis of Reinforced Concrete Shear Walls

Théorie de plasticité appliquée aux voiles en béton armé

Anwendung der Plastizitätstheorie auf Wände aus Stahlbeton

P. MARTI
Research Associate
Swiss Federal Institute of Technology
Zurich, Switzerland

SUMMARY
A review is given on recent attemps to establish a general theory of plane stress in reinforced concrete based on the theory of plasticity. Yield criteria for reinforced concrete wall elements are discussed and some applications to reinforced concrete shear walls are presented.

RESUME
Un aperçu est donné de quelques travaux récents basés sur la théorie de la plasticité, devant conduire à une théorie générale de l'état plan de contrainte dans des éléments en béton armé. Des critères d'écoulement pour des voiles en béton armé sont discutés et quelques applications sont présentées.

ZUSAMMENFASSUNG
Neuere plastizitätstheoretische Arbeiten werden besprochen, die sich mit einer allgemeinen Theorie des ebenen Spannungszustandes in Stahlbetonelementen befassen. Fliessbedingungen für Stahlbetonscheiben werden diskutiert, und einige Anwendungen auf Schubwände aus Stahlbeton werden angegeben.

1. INTRODUCTION

Shear walls in buildings are primarily designed to resist the effects of lateral forces due to wind or earthquake actions. Furthermore they are often also used to carry vertical loads. Apart from sufficient strength shear walls should provide appropriate stiffness for an acceptable behaviour under wind action and sufficient ductility to secure the integrity of the wall during several cycles of elastic-plastic deformation in an earthquake. The latter two problems are beyond the scope of the present paper. Only questions concerning the static strength of reinforced concrete shear walls are considered in the following. The discussion is further confined to recent applications of the theory of perfectly plastic bodies to such structural elements.

A typical example is shown in Fig. 1. Vertical and lateral loads are transfered to the shear walls by combined bending and membrane action of the floor slabs. Thus, each wall is subjected to combined bending, shear and axial forces. The individual shear walls may act together with the other structural elements. A portion of the total bending moment and axial force may be resisted by flange action of the transverse walls located at the edges of each shear wall. Acting as membranes the floor slabs may provide an external stirrup effect on the walls.

By means of simple truss models for each structural element a picture of the general mode of force transfer within and between the different elements of relatively complex systems similar to Fig. 1 can be obtained. Indeed, similar models are wellknown for applications to problems of shear transfer in reinforced concrete beams since the time of Ritter and Mörsch some seventy years ago. The extension to more general cases of plane stress conditions like those present in shear walls does not give rise to basically new problems. The truss model concept may be considered as a typical engineering approach which essentially coincides with the lower-bound method of limit analysis. Truss models, however are not able to reflect the kinematics of the collapse mechanisms of reinforced

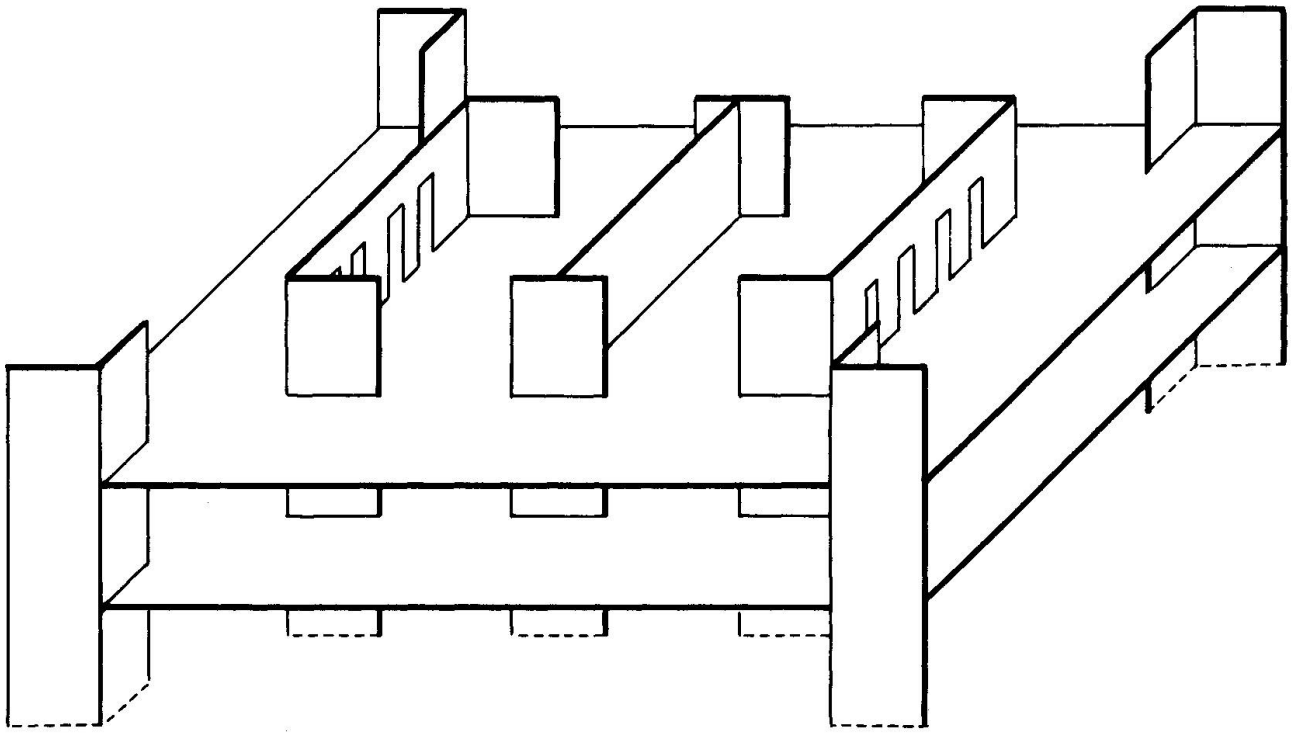

Fig. 1 Shear Walls in High-Rise Building

concrete beams or walls. Furthermore, local conditions e.g. the stress distribution at points of application of concentrated loads or reactions cannot be discussed in detail.

Recently attempts have been made to establish a general theory of plane stress in reinforced concrete based on the classical theory of plasticity. The purpose of the present paper is to review these developments. Yield criteria for reinforced concrete wall elements are discussed and some applications to reinforced concrete shear walls are presented. For simple problems exact solutions for the collapse load are obtained. In more general cases the methods of limit analysis allow to calculate lower and upper bounds for the collapse loads. Again, simple truss models prove to be helpful for constructing statically admissible stress fields according to the lower-bound method.

2. YIELD CRITERIA FOR REINFORCED CONCRETE WALL ELEMENTS

2.1 Assumptions

The investigation is based on the theory of perfectly plastic bodies in particular on the concept of plastic potential and the theorems of limit analysis.

The following assumptions are made:

1. The concrete is in a state of plane stress. It is a rigid-perfectly plastic material governed by a modified Coulomb yield criterion with associated flow rule.
2. The reinforcement is idealized as rigid-perfectly plastic with yield stresses $\pm f_y$. The bars carry forces in axial directions only. The distribution of the reinforcement is such that its action may be described by average stresses over the thickness of the wall (smeared reinforcement).
3. Local and bond failures are excluded.

2.2 Concrete

Coulomb's law of failure states that plastic flow occurs if the shear stress τ and the normal stress σ acting on any element in the material satisfy the linear equation

$$\tau + \sigma \cdot \tan\varphi - c = 0 \; . \qquad (1)$$

c and φ denote the cohesion and the angle of internal friction, respectively. The ratio between the uniaxial tensile and compressive strengths is

$$\zeta = \frac{1-\sin\varphi}{1+\sin\varphi} \; .$$

As shown by Shield [1] Coulomb's yield surface is an irregular hexagonal pyramid in principal stress space. The boundary planes are determined by the equations

$$\sigma_i \cdot (1+\sin\varphi) - \sigma_j \cdot (1-\sin\varphi) - 2 \cdot c \cdot \cos\varphi = 0 \; , \qquad i \neq j. \qquad (2)$$

For problems of bearing capacity of concrete blocks or rock Chen and Drucker [2] introduced a modified Coulomb yield criterion by assuming a small tensile strength

$$\sigma = f_t \geq 0 \; . \qquad (3)$$

This modified criterion consisting of the two conditions (1) and (3), i.e. a material description with three constants, is taken as a basis for the further treatment. In Fig. 2 the yield criterion is represented in the stress plane (a) and in the principal stress space (b) for $\sigma_3 = 0$ (plane stress).

For the application of limit analysis concrete is often assumed to have zero tensile and finite compressive strength. According to this assumption the yield locus DEFGHI in plane stress, Fig. 2 (b), is reduced to the wellknown square yield criterion ODEF. Nielsen [3], [4], Müller [5] and Clyde [6] treated the problem of plane stress in reinforced concrete wall elements using the square yield criterion. Considering the brittleness and the actual strain-softening property of concrete in compression the assumption of perfectly plastic behaviour is somewhat questionable. Nevertheless, this drastic idealization may well be taken as a basis for the calculation of collapse loads of reinforced concrete beams and walls. It is only necessary to take the limited ductility of concrete into account by choosing an effective value f_c which is reduced in comparison with the ordinary compressive strength measured e.g. on cylinders, [5], [7], [8], [9], [10]. The value f_c of the so-called effective concrete compressive strength may be interpreted as the average failure stress in a particular strain range depending on the problem under consideration. The magnitude of f_c must be determined by tests. The concept of an effective strength or yield stress level in connection with the application of the theory of plasticity is not new. In fact it is widely used in soil mechanics [17].

For some applications of limit analysis to plain and reinforced concrete elements the disregard of the concrete tensile strength is too restrictive. The square

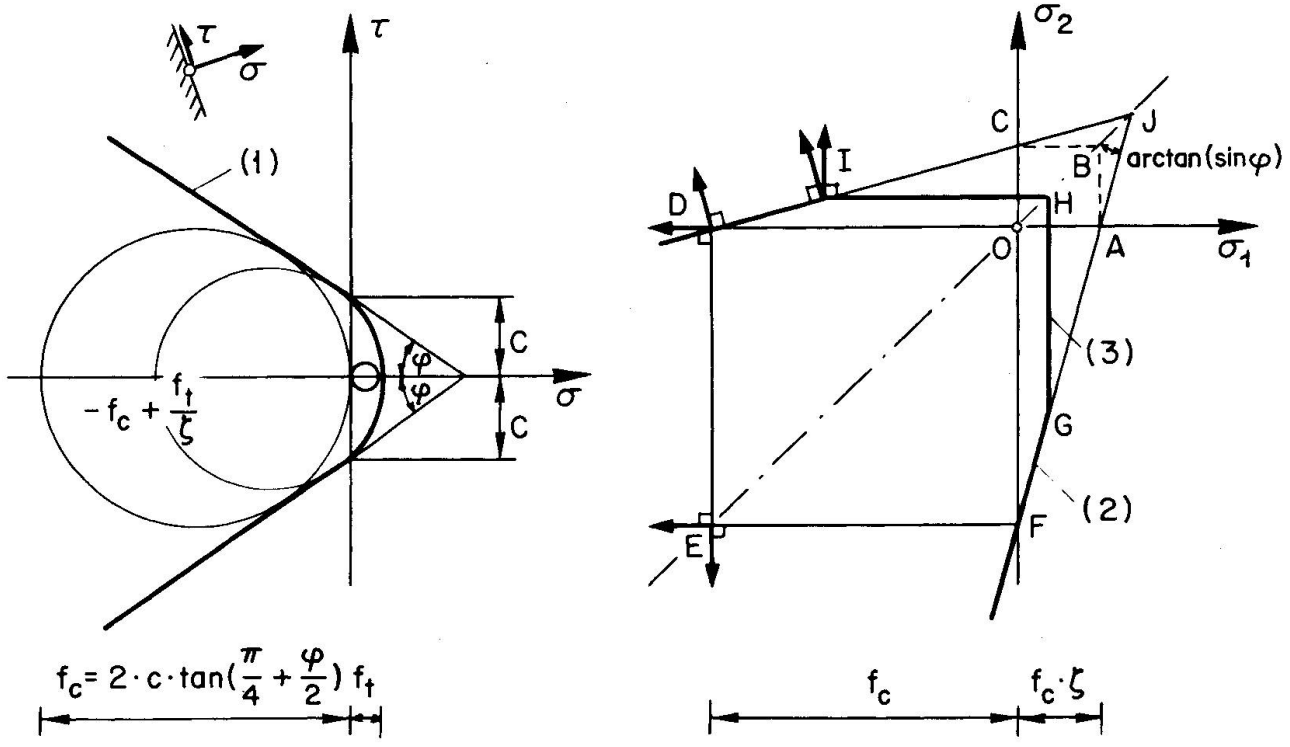

(a) Stress Plane (b) Principal Stress Space

Fig. 2 Coulomb's Yield Criterion

yield criterion is then replaced by a more general one, e.g. the modified Coulomb yield criterion applicable to plane strain as well as general stress states. Jensen [11] used the modified Coulomb yield criterion to analyse selected problems of plain and reinforced concrete. Braestrup et. al. [12] used the same criterion to determine upper bounds for the load producing axisymmetric punching of a reinforced concrete slab. Marti and Thürlimann [13] treated problems of plane stress and plane strain in reinforced concrete by using the unmodified Coulomb yield criterion, i.e. two material constants for the concrete only. As mentioned in [13], too high deviatoric stresses are obtained for higher hydrostatic pressures whereas the idealization might be reasonable e.g. in the tension-compression domains for plane stress condition. To avoid these deficiencies the use of the modified Coulomb yield criterion along with a realistic value for the angle of internal friction φ as a third material constant was suggested.

2.3 Reinforcement

A set of reinforcing bars parallel to axis η inclined at angle ϑ to the x-axis is considered, Fig. 3 (a). According to assumption 2 the action of the reinforcement can be described by the average stress

$$z_\eta = \mu_\eta \cdot \sigma_s \quad , \quad |z_\eta| \leq \mu_\eta \cdot f_y \quad . \tag{4}$$

μ_η and σ_s denote the reinforcement ratio and the stress in the bars, respectively. Transformation of the uniaxial stress state Eq. (4) to the orthogonal coordinates x and y yields the average stresses

$$z_x = z_\eta \cdot \cos^2\vartheta \quad , \quad z_y = z_\eta \cdot \sin^2\vartheta \quad , \quad z_{xy} = z_\eta \cdot \sin\vartheta \cdot \cos\vartheta \quad . \tag{5}$$

These stresses are taken as vector components in the stress space Fig. 3 (b). By linear combination of all possible stress states in the ξ- and η-reinforcements the parallelogram-shaped domain BDFH for the skew mesh is obtained. The extension to cases with more than two reinforcement directions is obvious. If the contribution of the compression reinforcement is neglected, e.g. [5], [10], the shaded domain OABC results.

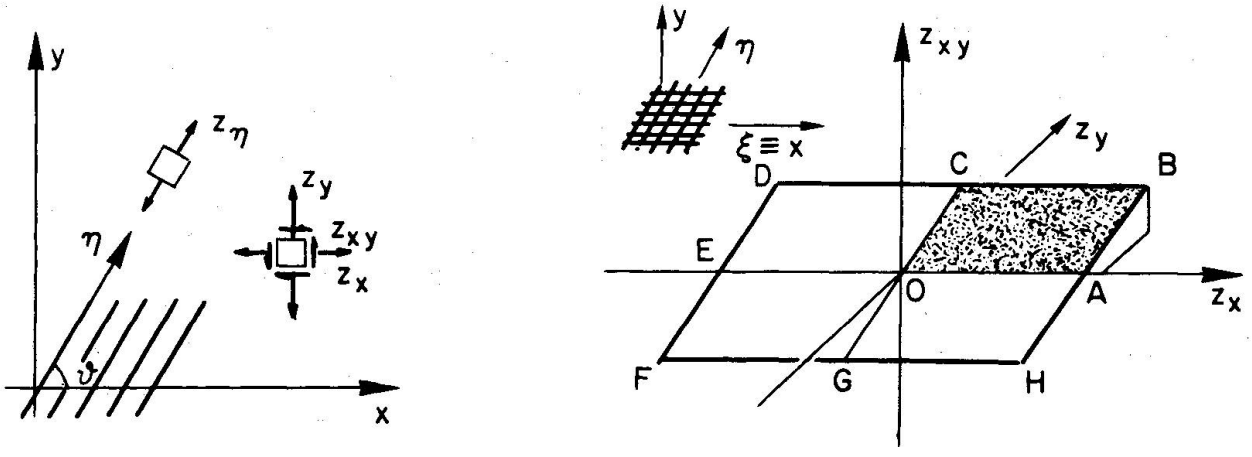

(a) Average Stresses (b) Yield Locus for Skew Mesh

Fig. 3 Yield Criterion for Reinforcement

2.4 Reinforced Concrete

Consider a differential wall element of reinforced concrete, Fig. 4. The thickness is taken equal to unity. The element is subjected to the membrane stresses N_x, N_y and N_{xy}. According to assumption 3 the bond between reinforcement and concrete is preserved until collapse. Therefore, the plastic strain increments or strain rates at collapse are equal for reinforcement and concrete. Hence, the yield surface in the stress space $\{N_x, N_y, N_{xy}\}$ is the envelope of all linear combinations

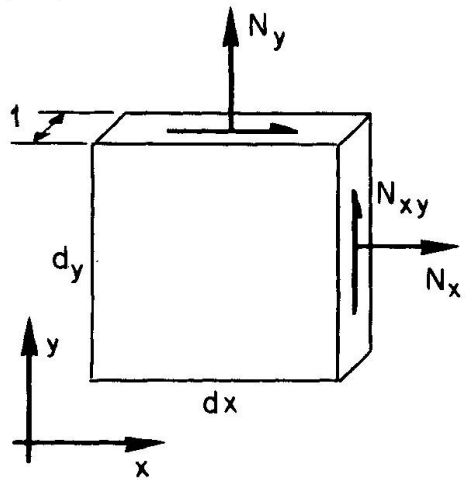

Fig. 4 Differential Wall Element

$$\begin{aligned} N_x &= n_x + z_x, \\ N_y &= n_y + z_y, \\ N_{xy} &= n_{xy} + z_{xy}, \end{aligned} \tag{6}$$

of stresses $\{n_x, n_y, n_{xy}\}$ and $\{z_x, z_y, z_{xy}\}$ which do not violate the yield criteria for the concrete and the reinforcement, respectively.

The modified Coulomb yield surface assumed for concrete is represented in Fig. 5. It consists of the three elliptical cones

$$\begin{aligned} &\text{I} \quad : \quad n_{xy}^2 - (f_t - n_x)\cdot(f_t - n_y) = 0, \\ &\text{II} \quad : \quad n_{xy}^2 - [\zeta\cdot(f_c + n_y) - n_x]\cdot[\zeta\cdot(f_c + n_x) - n_y]\cdot\frac{1}{(1+\zeta)^2} = 0, \\ &\text{III} \quad : \quad n_{xy}^2 - (f_c + n_x)\cdot(f_c + n_y) = 0. \end{aligned} \tag{7}$$

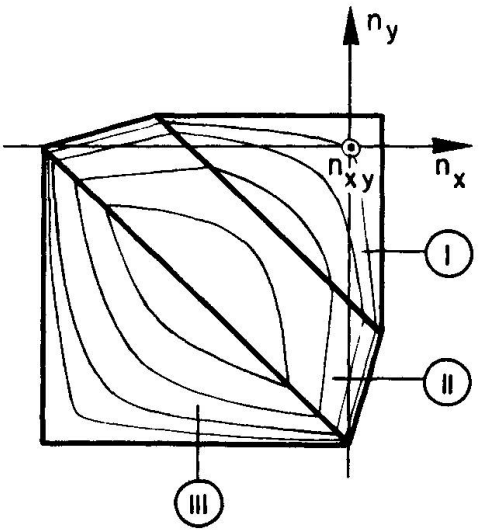

Fig. 5 Yield Surface for Concrete in Plane Stress

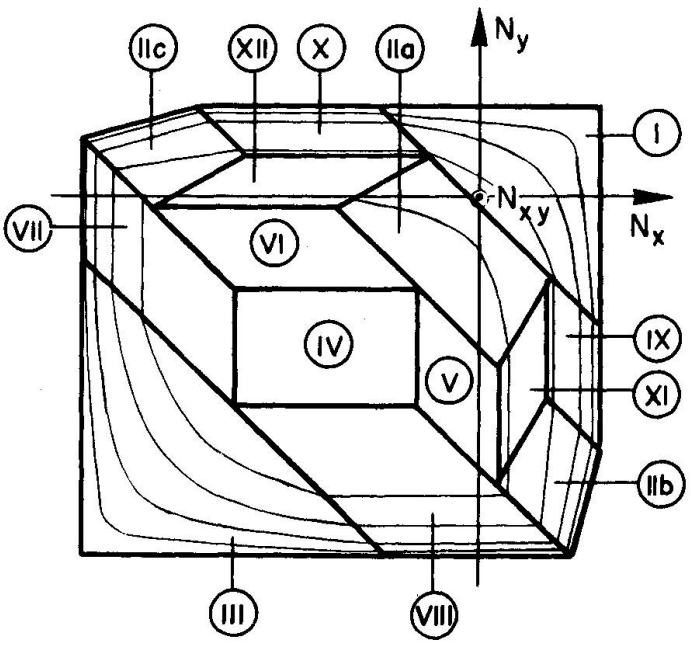

Fig. 6 Yield Surface for Orthogonally Reinforced Wall Element

According to Eq. (6) the yield surface for the reinforced concrete wall element may be obtained by simple translation of the yield surface for concrete, Eqs. (7), with the origin moved within the yield surface for the reinforcement. In Fig. 6 the resulting yield surface is represented for an element reinforced in the two orthogonal directions x and y. The cone II is split into three pieces. The two cones I and III are simply shifted. New yield regimes are created, viz. the planes IV, XI and XII and the circular cylinders V-X. The anisotropy of the yield criterion is obvious.

The stress states in the concrete and in the reinforcement for each yield regime may easily be visualized by means of simple geometrical considerations. As indicated in [13], where Coulomb's yield criterion was assumed for concrete, the detailed description of the different yield regimes given in that paper can be extended to the case of Fig. 6 without further difficulties. It is to be noted that for the yield regimes V-XII the reinforcements in one and for regime IV the reinforcements in both directions do not yield.

Except for several special cases the yield surface of Fig. 6 is of rather theoretical interest. In particular it should not be applied uncritically to plain concrete. In fact for most practical applications in reinforced concrete it will be judicious to neglect the concrete tensile strength and to provide a well distributed minimum reinforcement even in areas, where theoretically no reinforcement is necessary.

If the concrete tensile strength is neglected the yield regimes II and IX-XII disappear. In this form the yield criterion was derived for the first time by Nielsen [3] in the case of isotropic reinforcement. For low degrees of reinforcement say $\mu \cdot f_y / f_c < 0.1$ he suggested the use of an approximate yield surface composed of the two cones I and III, where f_t in Eq. (7) is replaced by $\mu \cdot f_y$. The kinematic aspects for isotropic walls governed by this yield criterion and the associated flow rule were discussed in [4]. In this thesis various exact solutions for isotropic walls (deep beams) and methods for the technical calculation of walls were presented. Müller [5] treated the yield criterion under the assumption of zero concrete tensile strength for arbitrary reinforcement and investigated the general stress and velocity fields in walls which are possible for the different yield regimes. For orthogonally reinforced elements the same yield criterion was also given by Clyde [6] in an attempt to reconcile recent developments such as the space truss model and the skew bending approaches in the theory of shear, torsion and bending of reinforced concrete beams. In theoretical accordance with the aforementioned references Clark [14] presented design equations for proportioning skew or orthogonal reinforcement to resist given membrane forces and suggested limits to the applicability of mild and high-strength steel as compression reinforcement.

2.5 Flow Rule and Velocity Discontinuities

According to the concept of plastic potential the plastic strain rates ε_x, ε_y and γ_{xy} are given by the flow rule

$$\varepsilon_x = \sum_{k=1}^{n} \frac{\partial \Phi_k}{\partial N_x} \cdot \lambda_k \,, \qquad \varepsilon_y = \sum_{k=1}^{n} \frac{\partial \Phi_k}{\partial N_y} \cdot \lambda_k \,, \qquad \gamma_{xy} = \sum_{k=1}^{n} \frac{\partial \Phi_k}{\partial N_{xy}} \cdot \lambda_k \,, \tag{8}$$

$$\lambda_k = 0 \text{ if } \Phi_k < 0, \qquad \lambda_k \geq 0 \text{ if } \Phi_k = 0 \,,$$

where the yield criterion is determined by n functions $\Phi_k(N_x, N_y, N_{xy}) \leq 0$.

Application of Eqs. (8) to the different yield regimes of Fig. 6 shows that one of the two strain rates ε_x and ε_y vanishes for the regimes V-XII and that $\varepsilon_x = \varepsilon_y = 0$ for regime IV. This is the kinematic interpretation of the above statement that one or both reinforcements do not yield. It is further to be noted that the principal directions for the plastic strain rates coincide with those of the stress state in the concrete but deviate in general from those of the membrane stresses $\{N_x, N_y, N_{xy}\}$.

For many actual collapse mechanisms the velocity fields are found to be discontinuous. Furthermore lines of discontinuity for velocities often prove to be convenient in deriving upper bounds for the collapse load. Consider a narrow zone of homogeneous deformation with thickness $d \to 0$ between two rigid parts, Fig. 7(a). The direction of the relative velocity v between the two parts forms the angle α with the deforming zone. The principal strain rates indicated in Mohr's circle, Fig. 7(b), are

$$\varepsilon_1 = \frac{v}{2 \cdot d} \cdot (1+\sin\alpha), \quad \varepsilon_2 = -\frac{v}{2 \cdot d} \cdot (1-\sin\alpha) \quad . \tag{9}$$

The principal directions 1 and 2 bisect the angles between the parallel to the discontinuity, I, and the normal to the velocity direction, II. In these so-called slip-line directions pure shearing strain rates occur.

The kinematic conditions for the yield regimes I ($\varepsilon_1 > 0$, $\varepsilon_2 = 0$), II ($\varepsilon_2/\varepsilon_1 = -\zeta$) and III ($\varepsilon_1 = 0$, $\varepsilon_2 < 0$) restrict the possibilities for discontinuities to $\alpha = \pi/2$, φ and $-\pi/2$, respectively. All other cases $\pi/2 > \alpha > -\pi/2$ can be related to one of the remaining regimes and in particular to the lines of intersection of different regimes.

Discontinuity lines for velocities according to the present theory should not be confused with the actual cracks observed in tests. The directions of the latter

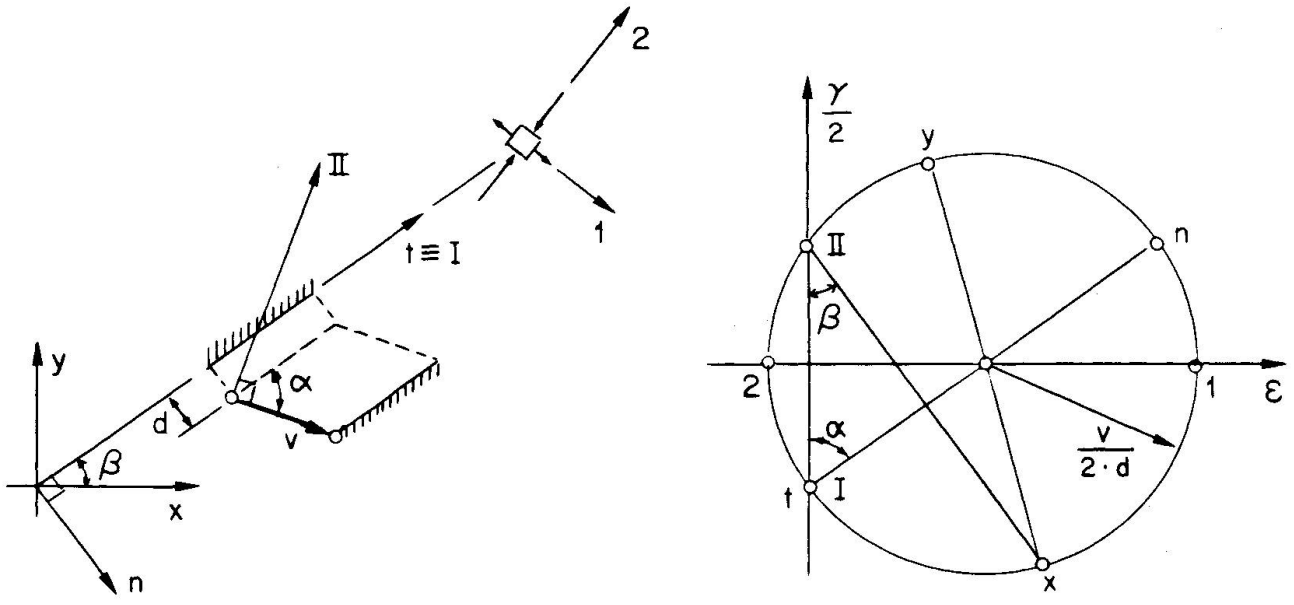

(a) Narrow Zone of Homogeneous Deformation (b) Strain Rates

Fig. 7 Line of Discontinuity for Velocities

tend towards the directions of the concrete compression trajectories at collapse. In contrast to this discontinuity lines or first slip lines may form angles up to $\pi/4$ with the principal directions in the concrete depending on the yield regime considered. Only for regime I ($\alpha = \pi/2$) a simple separation parallel to the concrete compression trajectories occurs. For this special case with coinciding slip lines the term "collapse crack" was introduced by Müller [5], [15].

2.6 Experimental Evidence

The redistribution of stresses predicted by plastic analysis is well confirmed experimentally for conditions corresponding to yield regime I of the presented yield criterion. Nielsen [4] gave a detailed review on available tests on reinforced concrete walls and deep beams. For reinforced concrete beams with thin-walled closed cross-section subjected to constant torsion and bending the existence of failure mechanisms which are compatible with the stress states assumed in space truss models was demonstrated by Müller [15], [5]. It can be deduced that the space truss models implicitely use yield regime I. Consequently, further confirmation of yield regime I is rendered by the generally observed good agreement between theory and experiments.

The experimental verification is not yet as well developed for the remaining yield regimes. It seems that presently the most evident indications can be obtained from the interpretation of shear tests on reinforced concrete beams, where the failure was initiated by web crushing. Recent investigations clearly demonstrate that the collapse loads and the failure mechanisms of such beams may well be predicted by plastic analysis provided that an appropriate concrete compressive strength f_c is assumed in the calculations [5], [7-10]. Müller [5] also found good agreement of his general theory of plane stress with tests on shear wall coupling beams reported by Paulay [16].

Much remains to do, however. The validity of the yield criterion should further be investigated. Minimum requirements for the detailing of the reinforcement should be established along with a better determination of the appropriate yield stress level or effective strength parameters.

3. APPLICATIONS TO SHEAR WALLS

3.1 Static and Kinematic Conditions, Exact Solutions

Referred to a Cartesian coordinate system a statically admissible stress field must satisfy the equilibrium conditions

$$\frac{\partial N_x}{\partial x} + \frac{\partial N_{xy}}{\partial y} + p_x = 0, \qquad \frac{\partial N_{xy}}{\partial x} + \frac{\partial N_y}{\partial y} + p_y = 0 \tag{10}$$

and the statical boundary conditions

$$t_x = N_x \cdot \cos\alpha + N_{xy} \cdot \sin\alpha, \qquad t_y = N_{xy} \cdot \cos\alpha + N_y \cdot \sin\alpha \; . \tag{11}$$

p_x and p_y are the components of the volume forces and t_x and t_y denote the components of the stresses on the boundary with its normal at an angle α to the x-axis.

If a strain rate field satisfies the compatibility condition

$$\frac{\partial^2 \varepsilon_x}{\partial y^2} + \frac{\partial^2 \varepsilon_y}{\partial x^2} - \frac{\partial^2 \gamma_{xy}}{\partial x \partial y} = 0 \qquad (12)$$

continuous velocities with components u and v exist for simply connected regions. The strain rates are determined by the equations

$$\varepsilon_x = \frac{\partial u}{\partial x} \quad , \quad \varepsilon_y = \frac{\partial v}{\partial y} \quad , \quad \gamma_{xy} = \frac{\partial u}{\partial y} + \frac{\partial v}{\partial x} \qquad (13)$$

and the velocities are obtained by integration. Apart from continuous fields discontinuities have often to be considered for exact as well as for upper-bound solutions, cf. section 2.5 above. Strain rate and velocity fields satisfying the compatibility conditions and the kinematic boundary conditions are termed kinematically admissible.

A stress field is said to be compatible with a strain rate field if the yield criterion and the flow rule are satisfied. For an exact solution a kinematically admissible strain rate field and a compatible, statically admissible stress field must be specified.

For each regime of the yield criterion, Fig. 6, and for all transitions in between the static and kinematic consequences for reinforced concrete walls can be treated separately. As an example the case of yield regime I is considered assuming zero concrete tensile strength. If volume forces p_x and p_y are neglected and the average stresses z_x and z_y due to the orthogonal reinforcement do not vary along the bars,

$$\frac{\partial z_x}{\partial x} = \frac{\partial z_y}{\partial y} = 0 \ ,$$

the equilibrium conditions Eqs. (10) reduce to

$$\frac{\partial n_x}{\partial x} + \frac{\partial n_{xy}}{\partial y} = 0 \quad , \qquad \frac{\partial n_{xy}}{\partial x} + \frac{\partial n_y}{\partial y} = 0 \quad . \qquad (14)$$

By using the stress function F,

$$n_x = - \frac{\partial^2 F}{\partial y^2} \ , \qquad n_y = - \frac{\partial^2 F}{\partial x^2} \ , \qquad n_{xy} = \frac{\partial^2 F}{\partial x \partial y} \ , \qquad (15)$$

Eq. (7) for yield regime I ($f_t = 0$) renders the differential equation

$$\frac{\partial^2 F}{\partial x^2} \cdot \frac{\partial^2 F}{\partial y^2} - \left(\frac{\partial^2 F}{\partial x \partial y} \right)^2 = 0 \qquad (16)$$

for all developable surfaces. Except for special cases (plane, cylindrical and conical surfaces) developable surfaces can be described by tangents to a space curve. Projection on the x-y-plane leads to a one-parametric set of straight lines and to their envelope. These straight lines, being the projected directions of zero principal curvature of F, are the compression trajectories of the concrete. Generally they form non-centered fans. The plastic deformation at collapse is a uniaxial straining directed at right angles to the concrete compression trajectories.

A detailed discussion covering all regimes for $f_t = 0$ is given in [5]. In particular it is found that the first slip lines are again straight and tangential to

an envelope for the regimes V-VIII for which the reinforcements in one direction do not yield, $\varepsilon_x = 0$ or $\varepsilon_y = 0$.

Few exact solutions have been developed so far. Nielsen [4] treated several examples of isotropic walls (deep beams). A direct application of the different regimes of the presented yield criterion is often obtained by idealizing the compression zone and the longitudinal reinforcement of reinforced concrete beams as stringers, i.e. bars with vanishing diameter and finite uniaxial strength. The webs, bounded by the stringers, are governed by the conditions of the appropriate yield regime. In this way coinciding lower- and upper-bound solutions have been derived for some problems [5], [9]. However, many questions require further clarification among others the conditions at points of application of concentrated loads or reactions.

Consider the rectangular wall element ACDF with the thickness taken equal to unity, Fig. 8 (a). Along AC and DF the element is bounded by two rigid parts. The element is subjected to the shear force V. The bending moment vanishes at midspan, x = a/2. The concrete is assumed to have zero tensile strength. Reinforcement is provided in the x-direction only ($\mu_x > 0$, $\mu_y = 0$). It is supposed to be placed symmetrically with respect to the straight line y = 1/2, e.g. con-

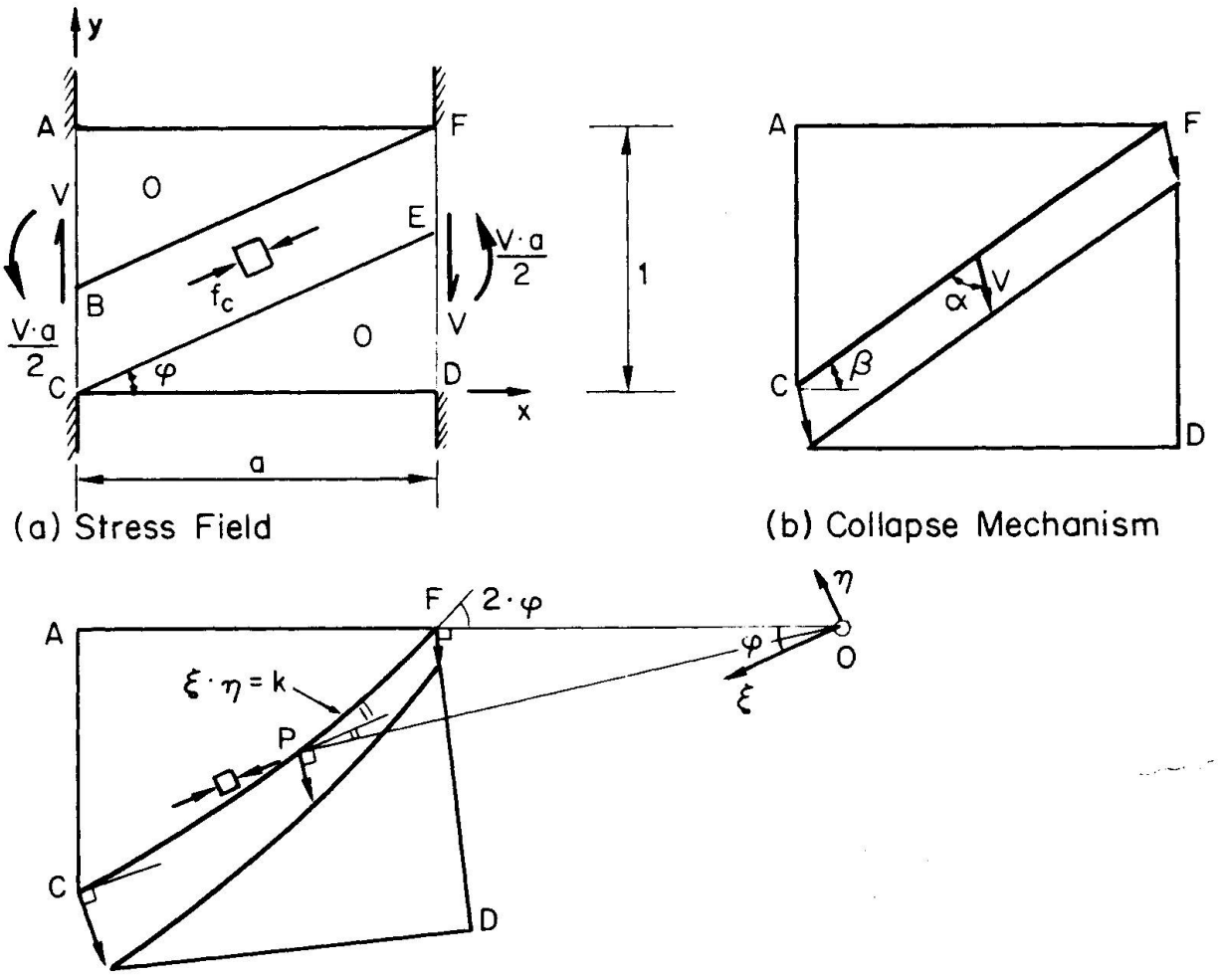

Fig. 8 Shear Transfer by Strut Action - No Shear Reinforcement

centrated at the edges AF and CD or/and uniformly distributed. With $\omega_x = \mu_x \cdot f_y / f_c$ the resistance of the reinforcement is related to the yield stress level of the concrete. The shear force is transfered by the concrete compression strut BCEF, inclined at angle φ to the x-axis. The lines BF and CE are discontinuity lines for the stress field. They separate the stress-free regions ABF and CDE from BCEF. The equilibrium conditions render

$$V = f_c \cdot \sin\varphi \cdot \cos\varphi \cdot (1 - a \cdot \tan\varphi) \tag{17}$$

and with $\beta = \operatorname{arccot} a$, Fig. 8 (b), for yielding reinforcement

$$\sin(2\cdot\varphi - \beta) = (1 - 2\cdot\omega_x)\cdot\sin\beta \quad . \tag{18}$$

For $\omega_x \geq .5$ the reinforcement does not yield and the angle φ and the shear force V remain constant:

$$2\cdot\varphi = \beta \quad , \qquad V = V_{max} = \frac{f_c}{2}\cdot\tan\left(\frac{\beta}{2}\right) \quad .$$

A kinematically admissible mechanism is shown in Fig. 8 (b). It is characterized by a jump of the velocity along the diagonal CF of the wall element. The work equation renders the least upper bound

$$V = \frac{f_c}{2} \cdot \left[\sqrt{4\cdot\omega_x\cdot(1-\omega_x) + a^2} - a\right] \tag{19}$$

for an angle α determined by

$$\cos(\alpha+\beta) = -(1 - 2\cdot\omega_x)\cdot\sin\beta \quad . \tag{20}$$

The upper-bound solution, Eq. (19), coincides with the lower-bound solution, Eq. (17). The direction of the concrete compression strut BCEF bisects the angle between the discontinuity line CF and the normal to the velocity: $2\cdot\varphi = \alpha + 2\cdot\beta - \pi/2$. For $\omega_x \geq .5$ the velocity v is parallel to the y-axis, $\alpha + \beta = \pi/2$, i.e. perpendicular to the non-yielding reinforcement. Fig. 8 (c) reflects the fact that the collapse mechanisms are not uniquely determined in general. An alternative mechanism is shown involving separation of the element along the hyperbola CPF and rotation of the rigid body CDF around the center of rotation O. As indicated in Fig. 8 (c) the direction of the concrete compression field bisects the angle between the tangent to the discontinuity line and the normal to the jump direction at an arbitrary point P. For the same collapse load, Eq. (19), an infinite number of mechanisms are possible with discontinuity lines lying between the limiting cases of Figs. 8 (b) and (c) and centers of rotation on the right-hand side of the element.

For the determination of the collapse load of reinforced concrete beams without shear reinforcement the stress field Fig. 8 (a) was already given by Drucker [18]. Nielsen et. al. [9] gave the complete lower- and upper-bound analyses leading to Eq. (19) for beams with rectangular cross-section subjected to a constant shear force V and reinforced in the longitudinal direction only. The mechanism Fig. 8 (c) is due to Müller [5]. He also investigated stress fields for combined shear transfer by strut action and shear reinforcement ($\mu_y > 0$) and found good agreement with tests on shear wall coupling beams reported by Paulay [16].

3.2 Lower-Bound Solutions

The static or lower-bound method of limit analysis requires the determination of a statically admissible stress field which nowhere violates the yield criterion. The corresponding loads are lower bounds for the actual collapse load.

The fundamental significance of the lower-bound theorem for design is evident. Based on equilibrium and yield considerations alone a safe structure can be designed. If a configuration is found to transfer given forces it is only necessary to keep the stresses everywhere below yield. An adequate proportioning of the structure as a whole and of its parts is achieved if the adopted force transfer system is consistently followed.

In principle, statically admissible stress fields for walls can be found by introducing a stress function F for the membrane stresses N_x, N_y and N_{xy} similar to that used in Eqs. (15) for the concrete stresses n_x, n_y and n_{xy}, viz.

$$N_x = -\frac{\partial^2 F}{\partial y^2} - \int p_x d_x, \qquad N_y = -\frac{\partial^2 F}{\partial x^2} - \int p_y d_y, \qquad N_{xy} = \frac{\partial^2 F}{\partial x \partial y} \quad . \tag{21}$$

Herewith the equilibrium conditions, Eqs. (10), are identically satisfied. The statical boundary conditions, Eqs. (11), determine the values of F and its first derivatives along the boundary of the wall. Thus, any function F satisfying the statical boundary conditions may be used as a stress function. Suitable numerical methods can be applied for the determination of the stresses. The reinforcement is then proportioned according to the principles outlined in section 2. Finally, the design may be improved by adjusting the stress distribution.

Although the described procedure is feasible and relatively simple its application will seldom be justified for practical design purposes. Still, for particular problems the use of simple continuous stress fields might be advantageous. For many practical problems, however, an approach using discontinuous stress fields will be sufficient. Therefore, two further methods of lower-bound analysis are indicated in the following, viz. the use of truss models and the construction of discontinuous stress fields.

From an engineering point of view it is often desirable to gain a simple picture of a discrete stress distribution within the continuous structure. Truss models of any kind are simple and adaptable systems for this purpose. Even for unusually complex geometrical and/or loading conditions a clear physical view of the mode of force transfer can be obtained. The forces acting in the truss members must be in equilibrium within the truss and with the external forces. If these members have sufficient strength all requirements for the application of the lower-bound theorem are fulfilled on the chosen level of idealization. Therefore, truss models render a sound basis for a safe design of structures.

A two stories high shear wall with I-shaped cross-section cut out of a building is shown in Fig. 9 together with the intermediate floor slab. Vertical and horizontal loads are acting on each story as indicated. Truss models are given for all structural elements. The resistance of the concrete and of the reinforcement is represented by compression and tension members, respectively. Distributed shear and normal forces acting in the web of the shear wall are transfered by simple strut action from story to story. Along the joint of the internal struts with the slab, the forces in the struts above and below are in equilibrium with the external forces transfered to these points by bending and membrane action of the slab. At the base of the outermost strut on the left side the vertical and the horizontal components of the strut force are taken by the compression flange

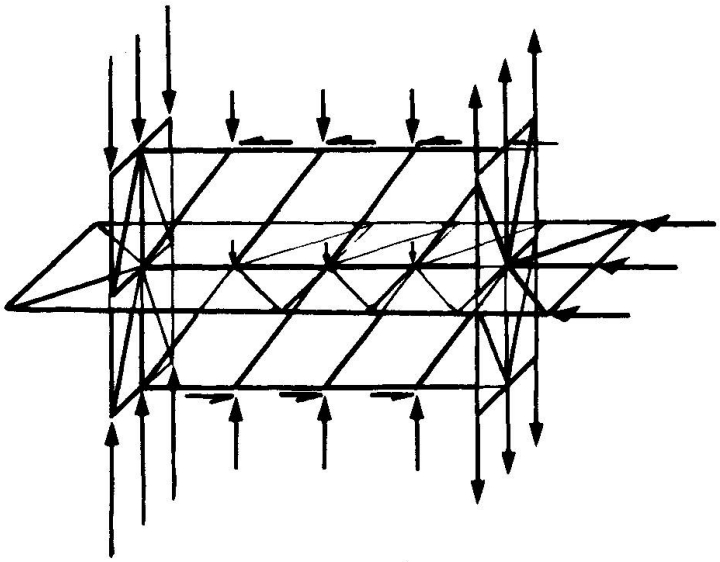

Fig. 9 Truss Models for Floor Slab and Flanged Shear Wall

and the slab on each story. Similarly, the reactions at the top of the outermost struts on the right side are taken by the tension flange and the floor slabs, respectively. The horizontal components of the outermost strut forces in the story above (left side) and below (right side) act on a truss in the plane of the floor slab. This truss consists of four tension members along the contour of the slab and of the compression diagonals connecting the corners of the slab with the points of load application at the junctions of web, flanges and slabs. From this truss action in the floor slabs an external stirrup effect results for the web of the shear wall. The transfer of the horizontal loads acting on the slab boundary is also indicated. Compression diagonals which meet at the connections of the internal struts in the web with the slab are tied together at their ends with transverse reinforcement in the slab. Similar considerations for both flanges allow to proportion their cross-sections and the required londitudinal and transverse reinforcements.

Local problems can be investigated using improved truss models with additional members. As an example the transfer of the vertical components of the strut forces in the web to the flanges in Fig. 9 is considered. In reality these forces will tend to be transfered continuously over the height of a story. Admissible stress distributions can be found. The favourable external stirrup effect of the slabs can again be used if a local reinforcement is provided over a certain width of the web along the flanges.

If the average axial stresses over appropriate cross-sections or widths of each member of the truss are kept below yield the dimensions of both concrete and reinforcement can be determined. Whereas generally this requirement is not too difficult to meet the conditions at the joints of the truss members require special examination. There, different uniaxial stress fields overlap. At the boundaries of the overlapping regions stress discontinuities occur with jumps of the normal stresses parallel to the discontinuity lines.

General configurations of discontinuous stress fields can be constructed if the widths of the truss members are gradually increased. Details of this technique are given elsewhere, e.g. [17]. As illustration a shear wall with rectangular cross-section is considered, Fig. 10. Along AD and EH the wall is bounded by floor slabs. The vertical and the horizontal loads transfered by the slab EH to the wall are acting uniformly distributed along EH and EG, respectively. Two uniaxial compression fields are assumed for the concrete, viz. the regions ABGH and ACEG. The overlapping region in the triangle ABG is bounded by the discontinuity lines AG and BG. Again, the floor slabs act as external stirrups. For example, the slab AD equilibrates the horizontal shear forces resulting along AB and CD in the walls above and below the slab, respectively. Only in the tension zone CDEF a uniformly distributed reinforcement is necessary. The average vertical stress due to this reinforcement is constant within the region CDEF between the

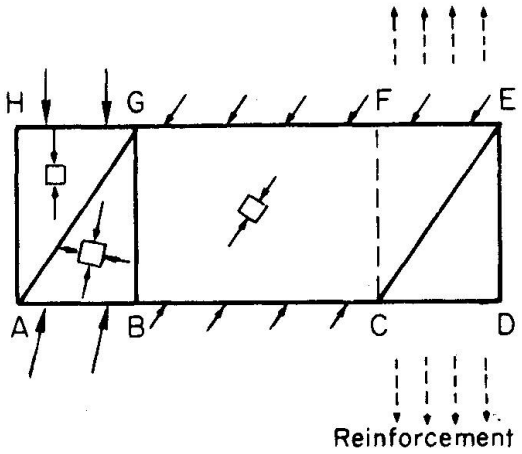

Fig. 10 Discontinuous Stress Field for Wall with Rectangular Cross-Section - No Shear Reinforcement

slabs. Along EF it changes by an amount equal to the vertical stress component of the inclined concrete compression field ACEG.

Lower-bound solutions using discontinuous stress fields were given by Nielsen [4] for rectangular walls with various loading and support conditions. Other frequently occuring types of walls, e.g. walls with openings, should similarly be investigated. The results should be checked by experiments and by complementary upper-bound analyses.

As for the examples considered above, theoretically no reinforcement will often be necessary in different areas of walls. However, the use of a well distributed minimum reinforcement throughout the walls is highly recommended in order to ensure the desired redistribution of stresses. Of course, no simple rule covering all possible cases can be given for the necessary amount of minimum reinforcement. In any case it will be of such an amount that a considerable contribution to the strength of the wall results. For economical reasons this extra strength should generally be taken into account.

The choice of the membrane stresses N_x, N_y and N_{xy} as generalized stresses implies some theoretical consequences so far not mentioned. The statical boundary conditions, Eq. (11), are satisfied in the form of generalized stresses, i.e. only for the sums of the stresses in the concrete and of the average stresses due to the smeared reinforcement, Eq. (6). Similarly, along a line of discontinuity only the sum of the normal and shear stresses acting on elements parallel to the discontinuity line must be continuous. The stresses in the concrete and in the reinforcement may have jumps which cancel each other. In both cases infinitely large bond stresses are theoretically required. According to assumption 3 in section 2.1 above such situations are not excluded. Actually, high stress concentrations may often occur. However, using a cautious design approach they will not endanger the overall strength in most practical applications. Still, more detailed information may be desirable. Therefore, problems of local stress distributions around the discrete reinforcing bars and problems of bond and local failures in general should further be investigated. It is felt that considerable progress can be obtained from a limit analysis approach using a suitable yield criterion for the concrete, e.g. a modified Coulomb criterion with appropriate yield stress levels.

3.3 Upper-Bound Solutions

Upper bounds for the actual collapse load are obtained from the work equation for an arbitrary, kinematically admissible velocity field. The work equation equates the external rate of work to the internal rate of dissipation computed from the flow rule, Eq. (8).

Compared with lower-bound solutions upper-bound analyses do not have the same direct applicability in practical design. They should rather be used to check the chosen dimensions. On the other hand, starting from the observed modes of failure, the upper-bound method may render excellent services for the interpretation of

tests.

Only one typical example is considered in the following. The rectangular wall element ABCD in Fig. 11(a) represents a shear wall with rectangular cross-section. As part of a building it is bounded by floor slabs along AB and CD which act as rigid external stirrups. The element is subjected to the bending moment M, the axial force N and the shear force V. The thickness of the wall is taken equal to unity.

A mechanism with a velocity discontinuity along the diagonal BD of the element is analysed. The relative velocity v between the two parts ABD and BCD is inclined at angle α to the discontinuity line. Obviously, this mechanism corresponds to that of Fig. 8 (b). Since an external axial compression force has the same effect on the concrete as an internal longitudinal reinforcement the shear force V in the unreinforced element is determined by Eq. (19) if the reinforcement ratio ω_x is replaced by $-N/f_c$. The corresponding interaction curve in Fig. 11 (c) is the circular line OAB. For the reinforced element the concept of linear combination outlined in section 2.4 can again be applied. In fact, the contributions of the reinforcements in x- and y-direction correspond in the work equation to those of the forces N and V, respectively. Thus, the curve CDEF is obtained by simple translation $\pm\ \omega_x$ in N-direction and the curve GHIJ if the action $\omega_y \cdot a$ of the shear reinforcement is added.

An unlimited increase of the ratio of shear reinforcement, ω_y, is of no use. For the mechanism Fig. 11 (b) the shear reinforcement does not yield, $\varepsilon_y = 0$. This mechanism may be considered as the special case a = 0 of the mechanism Fig. 11(a). Its interaction curve in Fig. 11 (c) for the unreinforced element is the half-circle OKB, which may also be interpreted as the projection parallel to the axis n_y of the yield surface for concrete ($f_t = 0$), Fig. 5, on the plane $\{n_x, n_{xy}\}$. Addition of longitudinal reinforcement gives the line CNLKMPF, the projection of the yield surface for reinforced concrete, Fig. 6, on the plane $\{N_x, N_{xy}\}$. For the chosen parameters a and ω_y the final interaction curve CNHIPF results.

Since only upper bounds for the collapse load were derived the possibility of a failure under combined bending and axial force should also be checked. In Fig. 11 (d) the exact interaction curve for the uniaxial stress state due to bending and axial force alone is again obtained by linear combination of the admissible stress states for concrete and steel. The yield locus for the unreinforced concrete is the parabola OAB with the equation

$$\frac{M}{f_c/2} + \left(\frac{N}{f_c} + \frac{1}{2}\right)^2 = \frac{1}{4} \quad .$$

If the longitudinal reinforcement is concentrated in halves along both edges of the element the yield locus CDE for the reinforcement results. This is the half of a square with diagonals of length $2 \cdot \omega_x$. If the reinforcement is uniformly distributed the inscribed parabola CFE with the equation

$$\frac{M}{f_c/2} \cdot 2 \cdot \omega_x + \left(\frac{N}{f_c}\right)^2 = \omega_x^2$$

is obtained. Linear combination of the yield locii OAB and CDE renders the final interaction curve CDGHI.

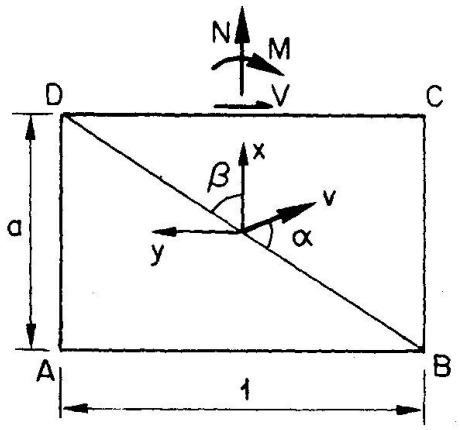

(a) Velocity Discontinuity

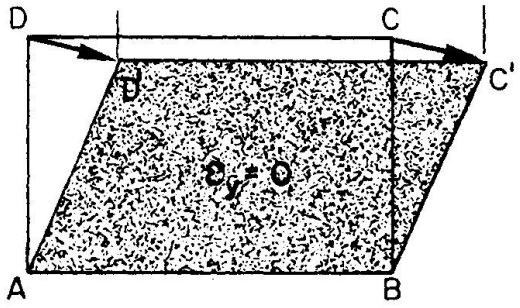

(b) Homogeneous Deformation

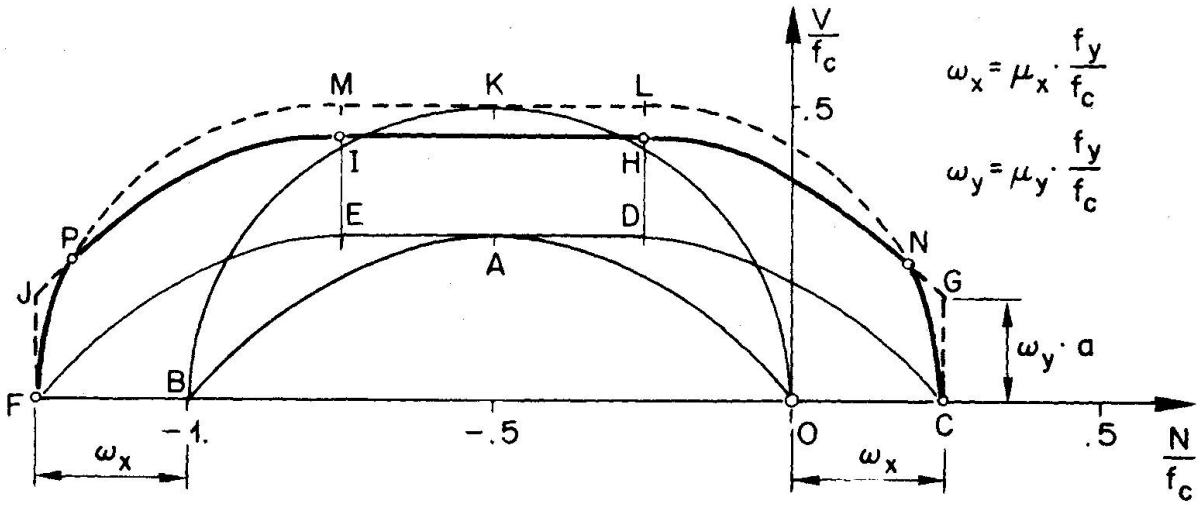

(c) Interaction Shear-Axial Force

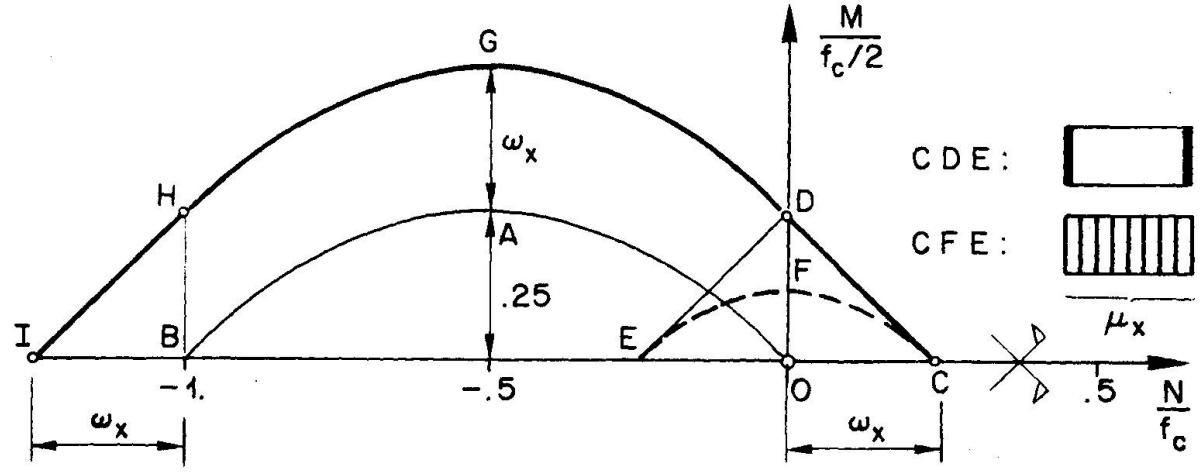

(d) Interaction Bending-Axial Force

Fig. 11 Upper-Bound Analysis for Shear Wall Element

REFERENCES

1 Shield, R.T.: "On Coulombs Law of Failure in Soils", Journal of the Mechanics and Physics of Solids, Vol. 4, 1955, pp. 10-16.

2 Chen, W.F. and Drucker, D.C.: "Bearing Capacity Problems of Concrete Blocks and Rock", Journal of the Engineering Mechanics Division, ASCE, Vol. 95, No. EM4, Aug., 1969, pp. 955-978.

3 Nielsen, M.P.: "Yield Conditions for Reinforced Concrete Shells in the Membrane State", Non-classical Shell Problems, Proc. IASS Symposium, Warsaw 1963. Amsterdam: North-Holland Publishing Company, pp. 1030-1040.

4 Nielsen, M.P.: "On the Strength of Reinforced Concrete Discs", Acta Polytechnica Scandinavica, Civil Engineering and Building Construction Series No. 70, 1971, p. 261.

5 Müller, P.: "Plastische Berechnung von Stahlbetonscheiben und -balken", Dissertation Nr. 6083, ETH Zürich, Institut für Baustatik und Konstruktion, ETH Zürich, Bericht Nr. 83, Birkhäuser Verlag Basel und Stuttgart, 1978.

6 Clyde, D.H.: "A General Theory for Reinforced Concrete Elements", Australasian Conference on the Mechanics of Structures and Materials, Christchurch New Zealand, Aug. 1977.

7 Braestrup, M.W.: "Plastic Analysis of Shear in Reinforced Concrete", Magazine of Concrete Research, Vol. 26, No. 89, Dec. 1974, pp. 221-228.

8 Nielsen, M.P. and Braestrup, M.W.: "Plastic Shear Strength of Reinforced Concrete Beams", Bygningsstatiske Meddelelser, Vol. 46, No. 3, Sept. 1975, pp. 61-99.

9 Nielsen, M.P., Braestrup, M.W., Jensen, B.C. and Bach, F.: "Concrete Plasticity", Danish Society for Structural Science and Engineering, Special Publication, Preliminary Manuscript, Dec. 1976.

10 Braestrup, M.W., Nielsen, M.P. and Bach, F.: "Plastic Analysis of Shear in Concrete", Danish Center for Applied Mathematics and Mechanics, No. 120, May 1977.

11 Jensen, B.C.: "Lines of Discontinuity for Displacements in the Theory of Plasticity of Plain and Reinforced Concrete", Magazine of Concrete Research, Vol. 27, No. 92, Sept. 1975, pp. 143-150.

12 Braestrup, M.W., Nielsen, M.P., Jensen, B.C. and Bach, F.: "Axisymmetric Punching of Plain and Reinforced Concrete", Technical University of Denmark, Structural Research Laboratory, Report R 75, 1976, p. 33.

13 Marti, P. and Thürlimann, B.: "Fliessbedingung für Stahlbeton mit Berücksichtigung der Betonzugfestigkeit", Beton- und Stahlbetonbau, Vol. 72, No. 1, Jan. 1977, pp. 7-12.

14 Clark, L.A.: "The Provision of Tension- and Compression Reinforcement to Resist In-Plane Forces", Magazine of Concrete Research, Vol. 28, No. 94, March 1976, pp. 3-12.

15 Müller, P.: "Failure Mechanisms for Reinforced Concrete Beams in Torsion and Bending", Institut für Baustatik und Konstruktion, ETH Zürich, Report No. 65, Reprint from IABSE Memoires, Vol. 36-II, Zürich 1976. Birkhäuser Verlag Basel und Stuttgart, 1976.

16 Paulay, T.: "The Coupling of Shear Walls", Thesis Univ. of Canterbury, Christchurch, New Zealand, 1969.

17 Chen, W.F.: "Limit Analysis and Soil Plasticity", Developments in Geotechnical Engineering Vol. 7, Elsevier, New York, 1975, p. 638.

18 Drucker, D.C.: "On Structural Concrete and the Theorems of Limit Analysis", IABSE Publications, Vol. 21, 1961, pp. 49-59.

Leere Seite
Blank page
Page vide

Plastic Analysis of Reinforced Concrete Beams

Analyse plastique des poutres en béton armé

Plastische Berechnung von Stahlbeton-Trägern

BRUNO THÜRLIMANN
Professor of Structural Engineering
Swiss Federal Institute of Technology
Zurich, Switzerland

SUMMARY

Plastic solutions for the strength of reinforced concrete beams under bending, shear, torsion and combined actions are presented. Associated problems of structural details are mentioned. Observations on a relevant comparison of theoretical values with experimental results are made. The practical use in specifications is indicated.

RESUME

Des solutions plastiques sont présentées pour déterminer la résistance ultime des poutres en béton armé soumises à la flexion, à l'effort tranchant, à la torsion et à des efforts combinés. Les détails constructifs correspondants sont également traités. La comparaison des valeurs théoriques avec les résultats expérimentaux donne lieu à quelques remarques. Une application pratique pour des normes est mentionnée.

ZUSAMMENFASSUNG

Plastische Lösungen für den Widerstand von Stahlbetonbalken unter Biegung, Schub, Torsion und kombinierter Beanspruchung werden dargestellt. Auf die entsprechenden konstruktiven Detailprobleme wird hingewiesen. Bemerkungen zu einem sinnvollen Vergleich von theoretischen Werten mit experimentellen Resultaten werden gemacht. Die praktische Anwendung in Normen wird erwähnt.

1. INTRODUCTION

The bending strength of reinforced concrete beams and slabs is determined by assuming a fully plastified stress distribution over the depth of the section. If the steel starts yielding considerably before crushing of the concrete (under reinforced sections), large plastic rotations will occur. Hence, the notions of "plastic hinge" (beams) and "yield line" (slabs) were introduced. The theory of plasticity can then be applied to calculate the collapse load of beams (one-dimensional) or slabs (two-dimensional).

However, the practical calculation of the strength of members subjected to torsion, shear and combined action is still based on rather crude semi-empirical formulas derived from test data.

This report gives a summary of results obtained during the past 10 to 15 years on the application of the theory of plasticity to such cases. In general, the three-dimensional extent of a beam must be taken into account making the analysis accordingly more complicated. Pertinent references are indicated and listed at the end.

2. SHEAR WEB

Beams with rectangular, box-, T-, H- or [-sections can be decomposed into their functional elements, namely flanges or corner stringers subjected to tension or compression and connecting web elements under pure shear. The strength of such a web element will hence be analyzed first ([1], [2], [3], [4]).

A web element subjected to a shear flow, $S = \tau d$, with an orthogonal reinforcement A_x, A_y is shown in Fig. 1. According to the plastic theory the following assumptions are made (Fig. 2):

1. Rigid-plastic material behaviour
2. Forces in the reinforcements only in axial direction, i.e. no shear resistance of the reinforcing net, no doweling action; yield values per unit with p_x, p_y.
3. Zero tensile strength for the concrete; square yield criterion with orthogonality of the plastic strain rates $\dot{\varepsilon}_1$, $\dot{\varepsilon}_2$ with the yield surface.

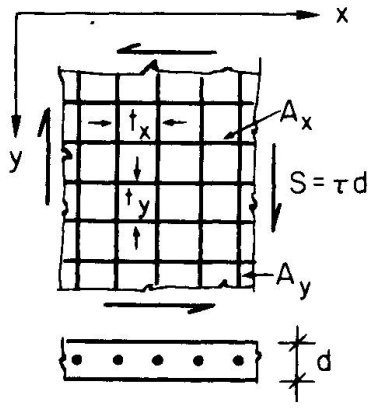

$$a_x = \frac{A_x}{t_y}\,; \qquad a_y = \frac{A_y}{t_x}\,;$$

$$p_x = a_x f_{sx} \qquad p_y = a_y f_{sx}$$

Fig. 1 Shear Web Element

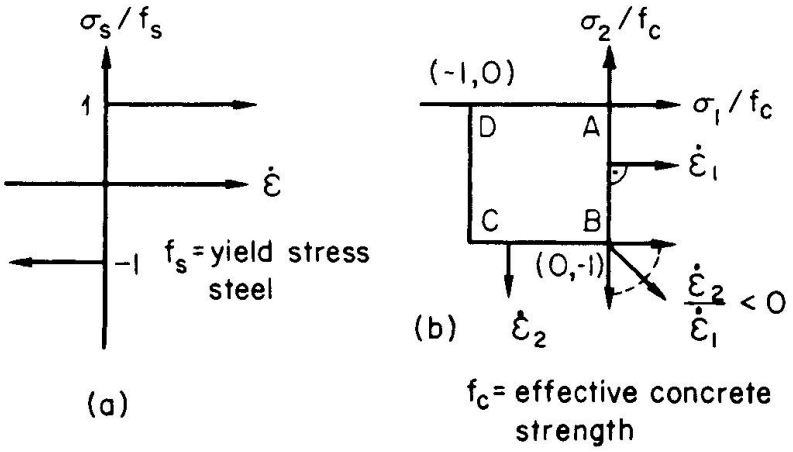

Fig. 2 Yield Criteria

Obviously all deformations up to the onset of unrestricted plastic flow are neglected. Especially previously formed cracks must have a sufficient aggregate interlock to transmit any forces necessary for a redistribution of the concrete stresses. The implication of these assumptions need to be discussed subsequently.

First, an admissible stress field is shown in Fig. 3. The concrete forms a diagonal compression field, $\sigma_1 = 0$, $\sigma_2 = \sigma_c$ under an angle α. The equality between the action $S = \tau d$ and the reactions requires

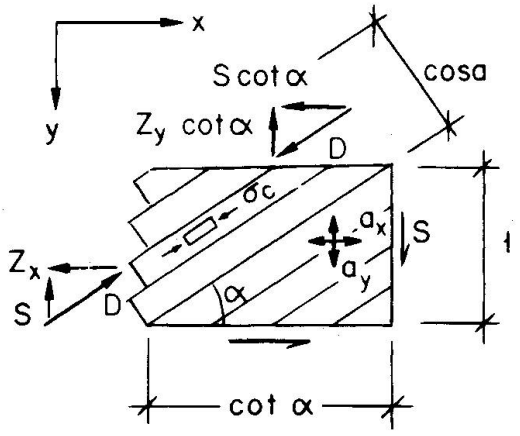

Fig. 3 Admissible Stress Field

$$D = -\sigma_c \cdot d \cdot \cos\alpha \qquad (1)$$

$$Z_x = D \cdot \cos\alpha = S \cdot \cot\alpha \qquad (2)$$

$$Z_y = S \cdot \tan\alpha \qquad (3)$$

Excluding first crushing of the concrete, hence $\sigma_c > -f_c$, the maximum value of the shear flow S_p is reached if both reinforcements yield

$$Z_x = p_x = S_p \cdot \cot\alpha$$

$$Z_y = p_y = S_p \cdot \tan\alpha \quad .$$

Solving for the two unknowns α and S_p gives

$$\tan^2\alpha = \frac{p_y}{p_x} = \lambda \qquad (4)$$

$$S_p = \sqrt{p_x \cdot p_y} = p_y\sqrt{\frac{1}{\lambda}} \qquad (5)$$

$$\sigma_c = -\frac{S_p}{d \cdot \sin\alpha \cdot \cos\alpha} = -\frac{p_y}{d}\left(1 + \frac{1}{\lambda}\right) \qquad (6)$$

$$\lambda = \frac{p_y}{p_x} \quad \text{(ratio of the yield forces)} \qquad (7)$$

For a fixed yield value p_y the yield force p_x can be increased till the strength

of the concrete is reached

$$-\sigma_c = f_c = \frac{p_y}{d}(1+\frac{1}{\lambda})$$

or

$$\lambda_c = \frac{p_y/f_c \cdot d}{1-p_y/f_c \cdot d} \tag{8}$$

Substituting into Eq. (5) gives the shear flow S_{pc} producing concrete failure

$$\frac{S_{pc}}{f_c \cdot d} = \sqrt{\frac{p_y}{f_c \cdot d}(1-\frac{p_y}{f_c \cdot d})} \tag{9}$$

The corresponding required yield force p_{xc} is

$$\frac{p_{xc}}{f_c \cdot d} = \frac{p_y}{f_c \cdot d}\cdot\frac{1}{\lambda_c} = 1-\frac{p_y}{f_c \cdot d} \tag{10}$$

Eqs. (9) and (10) are plotted in Fig. 4(a). Obviously, $p_x = p_y = 1/2 \cdot f_c \cdot d$ gives the maximum possible shear resistance with the inclination $\tan\alpha = 1$ of the concrete compression field. Keeping the total amount of reinforcement constant, $p_x + p_y = f_c \cdot d$, a distribution ratio $\lambda = p_y/p_x$ not equal to unity will diminish the shear resistance. For $p_y \to 0$ and $p_x \to 0$, the inclination reaches $\alpha = 0$ and $\pi/2$, respectively.

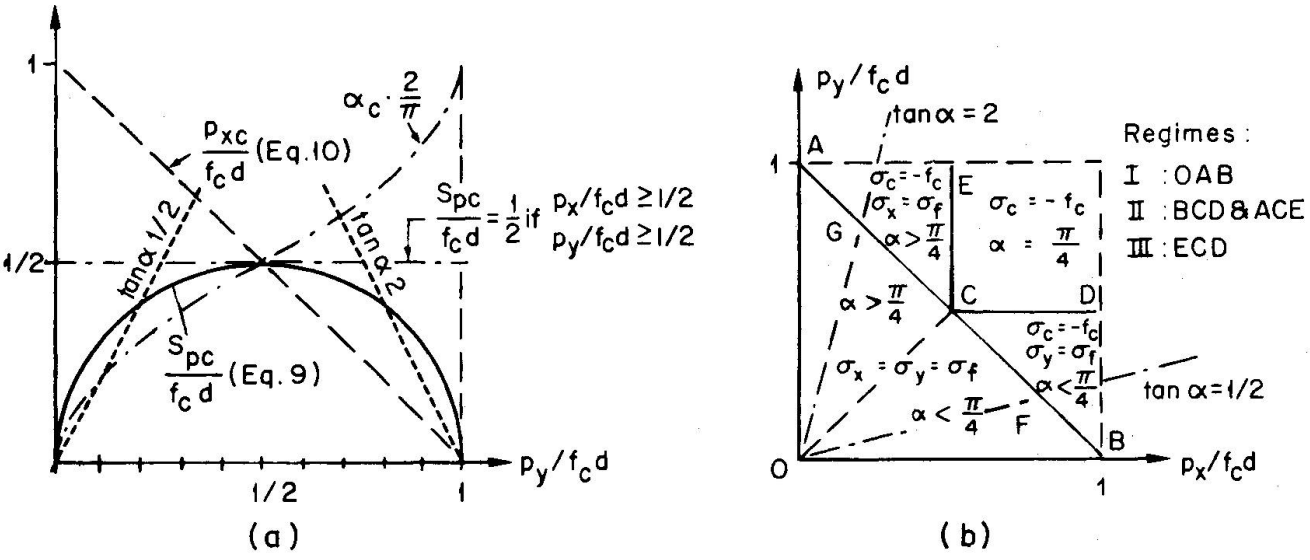

Fig. 4 Collapse Loads and Corresponding Regimes

An actual shear web will first crack at $\pi/4$. A redistribution of the concrete stresses such that extreme values α at collapse occur seems very unlikely. Hence, limiting values, $1/2 < \tan\alpha < 2$, have been proposed to exclude these extremes ([5], [6], [7]). The corresponding restriction is also shown in Fig. 4(a). A considerable reduction of the maximum concrete stresses for low values of $p_y/f_c \cdot d < 0.2$ (or $p_x/f_c \cdot d < 0.2$) are the desired consequence.

The corresponding kinematic solution is considered next. However, a discussion of kinematically admissible velocity fields is needed. In a band of thickness b,

Fig. 5, a linearly varying velocity field is assumed. With $\dot{w}_B$ the displacement rate from B to B' the values are

$$\dot{w} = \frac{\dot{w}_B}{b} \cdot n \tag{11}$$

$$\dot{w}_n = \frac{\dot{w}_B}{b} \cdot n \cdot \cos\vartheta \tag{12}$$

$$\dot{w}_t = \frac{\dot{w}_B}{b} \cdot n \cdot \sin\vartheta \tag{13}$$

and the strain rates

$$\dot{\varepsilon}_n = \frac{\partial \dot{w}_n}{\partial n} = \frac{\dot{w}_B}{b} \cdot \cos\vartheta \tag{14}$$

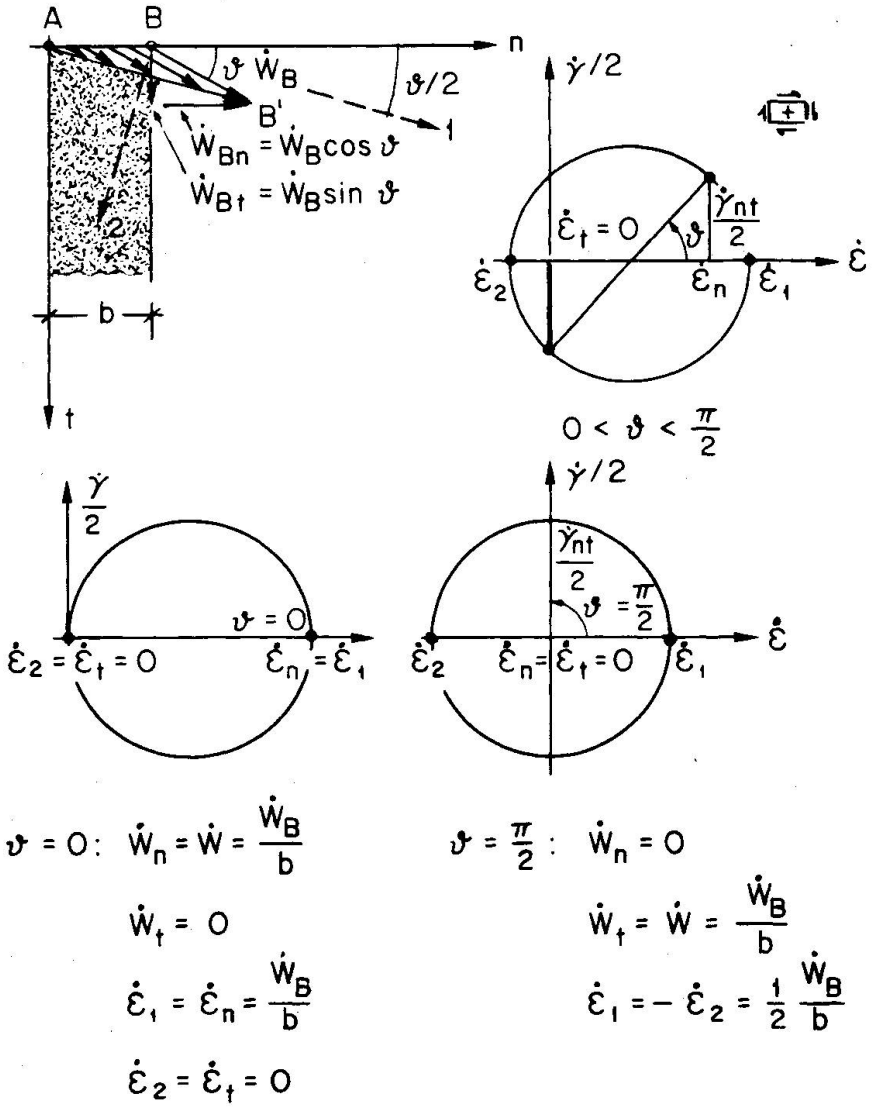

$\vartheta = 0$: $\dot{W}_n = \dot{W} = \frac{\dot{W}_B}{b}$

$\dot{W}_t = 0$

$\dot{\varepsilon}_1 = \dot{\varepsilon}_n = \frac{\dot{W}_B}{b}$

$\dot{\varepsilon}_2 = \dot{\varepsilon}_t = 0$

$\vartheta = \frac{\pi}{2}$: $\dot{W}_n = 0$

$\dot{W}_t = \dot{W} = \frac{\dot{W}_B}{b}$

$\dot{\varepsilon}_1 = -\dot{\varepsilon}_2 = \frac{1}{2}\frac{\dot{W}_B}{b}$

Fig. 5 Kinematics of Slip Bands

$$\dot{\varepsilon}_t = \frac{\partial \dot{w}_t}{\partial t} = 0 \tag{15}$$

$$\dot{\gamma}_{nt} = \frac{\partial \dot{w}_n}{\partial t} + \frac{\partial \dot{w}_t}{\partial n} = \frac{\dot{w}_B}{b} \sin\vartheta \tag{16}$$

Such a field is kinematically admissible as continuity over the band width b is provided. In particular, the strain $\dot{\varepsilon}_t = 0$.

The principal strain directions are indicated in a Mohr's circle, Fig. 5(b):

$$\dot{\varepsilon}_{1,2} = \frac{1}{2}(\dot{\varepsilon}_n + \dot{\varepsilon}_t) \pm \frac{1}{2}\sqrt{(\dot{\varepsilon}_n - \dot{\varepsilon}_t)^2 + \dot{\gamma}_{nt}^2} \tag{17}$$

$$\dot{\varepsilon}_1 = \frac{\dot{w}_B}{2 \cdot b}(1 + \cos\vartheta) \tag{18}$$

$$\dot{\varepsilon}_2 = \frac{\dot{w}_B}{2 \cdot b}(-1 + \cos\vartheta) \tag{19}$$

$$\tan\vartheta = \frac{\dot{\varepsilon}_n - \dot{\varepsilon}_t}{\dot{\gamma}_{nt}} = \frac{\dot{\gamma}_{nt}}{\dot{\varepsilon}_n} \tag{20}$$

The principal direction 1 forms an angle $\vartheta/2$ with the n-axis, hence, it always bisects the angle ϑ between the displacement rate $\dot{w}_B$ and the n-axis as shown in the figure.

The flow rule for concrete (Fig. 2) will now determine the angle ϑ at which $\dot{w}_B$ becomes possible.

Case A-B:

A stress point ($\sigma_1 = 0$; $0 < \sigma_2 < -f_c$) on A-B requires a strain rate $\dot{\varepsilon}_1 > 0$ and $\dot{\varepsilon}_2 = 0$. From Eq. (19) the condition is

$\cos\vartheta = 1 \rightarrow \vartheta = 0$

$\dot{w} = \dot{w}_n$

$\dot{w}_t = 0$

Consequently, the crack band opens perpendicularly to the direction of the compression field. No energy is dissipated in the concrete along the crack

Case B:

A singularity exists at stress point B ($\sigma_1 = 0$; $\sigma_2 = -f_c$). The situation is indeterminate as combinations $\dot{\varepsilon}_2/\dot{\varepsilon}_1 < 0$ become possible. The corresponding situation is described in Fig. 5 with the two extreme cases $\vartheta = 0$ and $\vartheta = \pi/2$. Any situation in between is possible. This behaviour will be of interest when discussing cases, where the concrete stress reaches its strength value f_c.

The basis is now prepared to discuss the kinematic solution for the web element of Fig. 6. The two parts separate normally at the rate $\dot{w}_B$. Equating the internal and external work rates leads to

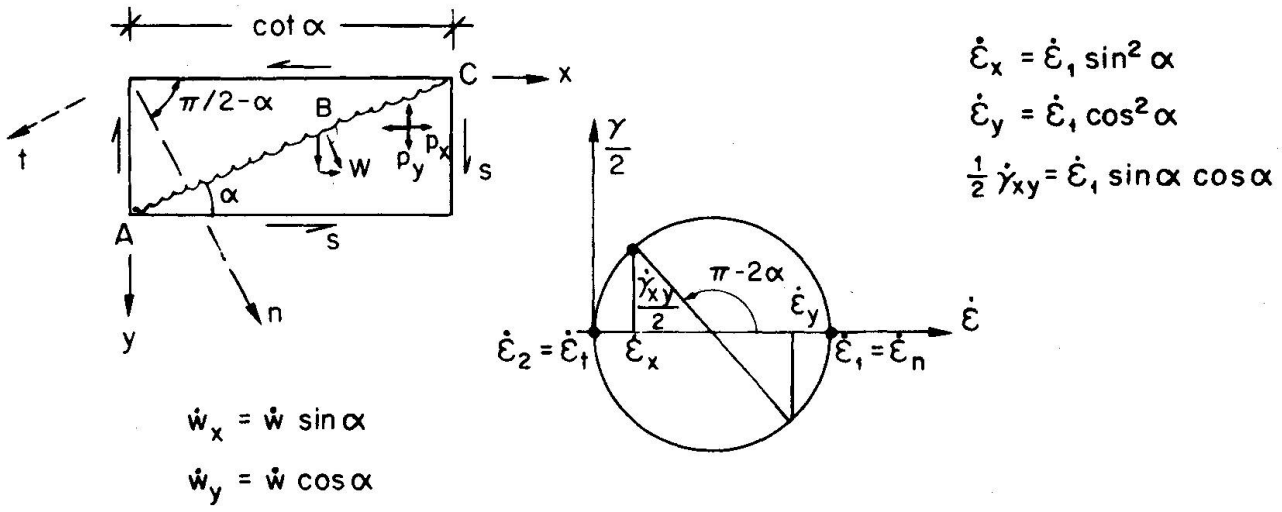

Fig. 6 Admissible Velocity Field

$$L_{in} = p_x \cdot \dot{w}_x + p_y \cdot \cot\alpha \cdot \dot{w}_y = L_{ex} = S \cdot \cot\alpha \cdot \dot{w}_x + S \cdot \dot{w}_y$$

Introducing the $\dot{w}$-values from Fig. 6

$$\dot{w}_x = \dot{w} \cdot \sin\alpha \,, \qquad \dot{w}_y = \dot{w} \cdot \cos\alpha \,, \qquad S = \frac{1}{2}(p_x \cdot \tan\alpha + p_y \cdot \cot\alpha) \,,$$

with the minimum value

$$\frac{\partial S}{\partial \alpha} = 0 = p_x \cdot \frac{1}{\cos^2\alpha} - p_y \cdot \frac{1}{\sin^2\alpha}$$

$$\tan^2\alpha = \frac{p_y}{p_x} = \lambda \qquad (21)$$

$$S_p = \sqrt{p_x \cdot p_y} = p_y \cdot \sqrt{\frac{1}{\lambda}} \qquad (22)$$

The solution coincides with the lower bound solutions Eq. (5). It should be noted that this kinematic solution does not give any information on the concrete stress σ_c.

The strain rates $\dot{\varepsilon}_x$, $\dot{\varepsilon}_y$ and $\dot{\gamma}_{xy}$ are related to $\dot{\varepsilon}_n = \dot{\varepsilon}_1$ as shown in Fig. 6

$$\dot{\varepsilon}_x = \dot{\varepsilon}_n \cdot \sin^2\alpha \,, \qquad \dot{\varepsilon}_y = \dot{\varepsilon}_n \cdot \cos^2\alpha \,, \qquad \dot{\gamma}_{xy}/2 = \dot{\varepsilon}_n \cdot \sin\alpha \cdot \cos\alpha \,.$$

In an actual shear web collapse will occur after considerable elastic and inelastic deformations have taken place. The above strain rate relations at collapse may, however, serve to estimate the total strains. Assuming

$$\frac{\varepsilon_{y\,tot}}{\varepsilon_{x\,tot}} \approx \frac{\dot{\varepsilon}_y}{\dot{\varepsilon}_x} = \cot^2\alpha \qquad (23)$$

$$\frac{\varepsilon_{n\,tot}}{\varepsilon_{x\,tot}} = \frac{\dot{\varepsilon}_y}{\dot{\varepsilon}_x} \approx \frac{1}{\sin^2\alpha} \qquad (24)$$

it follows that for small angles α, i.e. $p_y \to 0$, the $\varepsilon_{x\,tot}$ and $\varepsilon_{n\,tot}$ increase very rapidly. Even a small strain $\varepsilon_{x\,tot}$ below the yield strain of the longitudinal x-reinforcement will cause very large strains in the stirrup y-reinforcement and large cracks, $\varepsilon_{n\,tot}$ representing a "mean crack strain". Again, a limitation on the tolerable value of $\tan\alpha$ seems indicated in order to maintain the aggregate interlock across the cracks.

As previously discussed a mechanism in the form of a slip band will occur if strain rates $\dot{\varepsilon}_2 < 0$ become possible, hence, the concrete stress has reached its strength value $\sigma_c = -f_c$. According to Eqs. (11) and (12)

$$\dot{w}_n = \frac{\dot{w}_B}{n}\cdot\cos\vartheta \quad , \qquad \dot{w}_t = \frac{\dot{w}_B}{n}\cdot\sin\vartheta \quad ,$$

with the corresponding strain rates

$$\dot{\varepsilon}_1 = \frac{\dot{w}_B}{2\cdot b}(1+\cos\vartheta) \quad , \qquad \dot{\varepsilon}_2 = \frac{\dot{w}_B}{2\cdot b}(-1+\cos\vartheta) \quad , \qquad \tan\vartheta = \frac{\dot{\gamma}_{nt}}{\dot{\varepsilon}_n}$$

Referred to the compression field $\sigma_c = -f_c$ with an angle α in the x-, y-system, Fig. 7, the situation is illustrated for three cases. In the range $0 < \alpha < \pi/4$ the x-steel will cease to yield such that $\dot{w}_B = \dot{w}_y$. A slip band (S.B.) will then form under the angle 2α. Energy will now be dissipated by crushing of the concrete. The value of S_p will not change if the yield force p_x is increased over the critical value p_{xc} (Fig. 4(a)) just producing a concrete stress $\sigma_c = -f_c$.

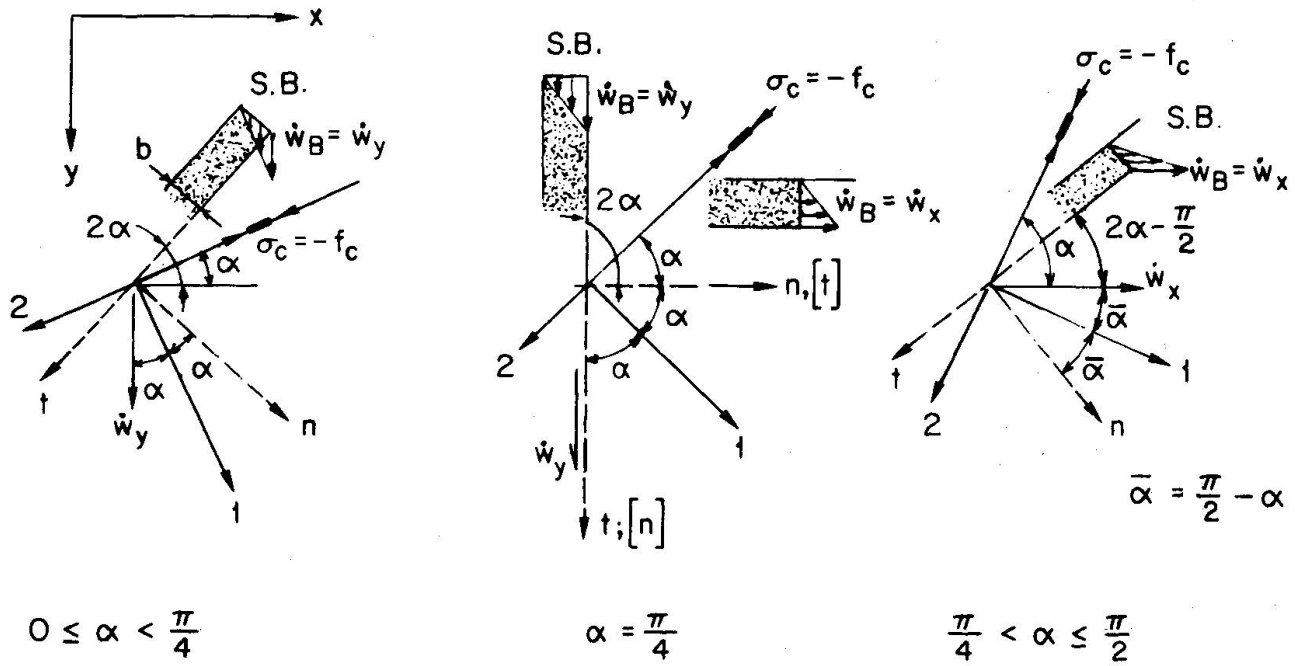

Fig. 7 Orientations of Slip Bands

If $\alpha = \pi/4$ the slip band will reach a vertical (or horizontal) position. Values $\pi/4 < \alpha < \pi/2$ occur if $p_x < p_y$. The slip band turns from the horizontal into the vertical position.

The finding are summirized in Fig. 4(b). Below line AB collapse is governed by yielding of both reinforcements. This yield regime will be termed Regime I. Beyond ECD failure occurs by crushing of the concrete without yielding of the steel (Regime III). In the two triangles AEC and CDB concrete and yielding of one reinforcement are controlling (Regime II). Hence, any increase of p_x in the triangle BDC or any increase of p_y in the triangle AEC will not change the value of S_p. For $p_x/f_c \cdot d = p_y/f_c \cdot d = 1/2$ the maximum possible resistance is reached. The limitations imposed by $1/2 < \tan\alpha < 2$ are cutting off the border regions OBF and OAG, respectively.
In the subsequent sections reference will be made to the three different yield regimes I, II and III defined above.

From a strength point of view the formation of slip bands does not give new information as indicated above. However, the slip mechanisms allow new kinematic configurations if external geometrical restraints are present. Furthermore, they may allow better physical explanations of test observations.

3. TORSION AND BENDING

In a box beam with rectangular cross section $b \cdot h$, Fig. 8, torsion produces a constant shear flow around the perimeter

$$S = \tau d = \frac{T}{2A_o} \qquad (25)$$

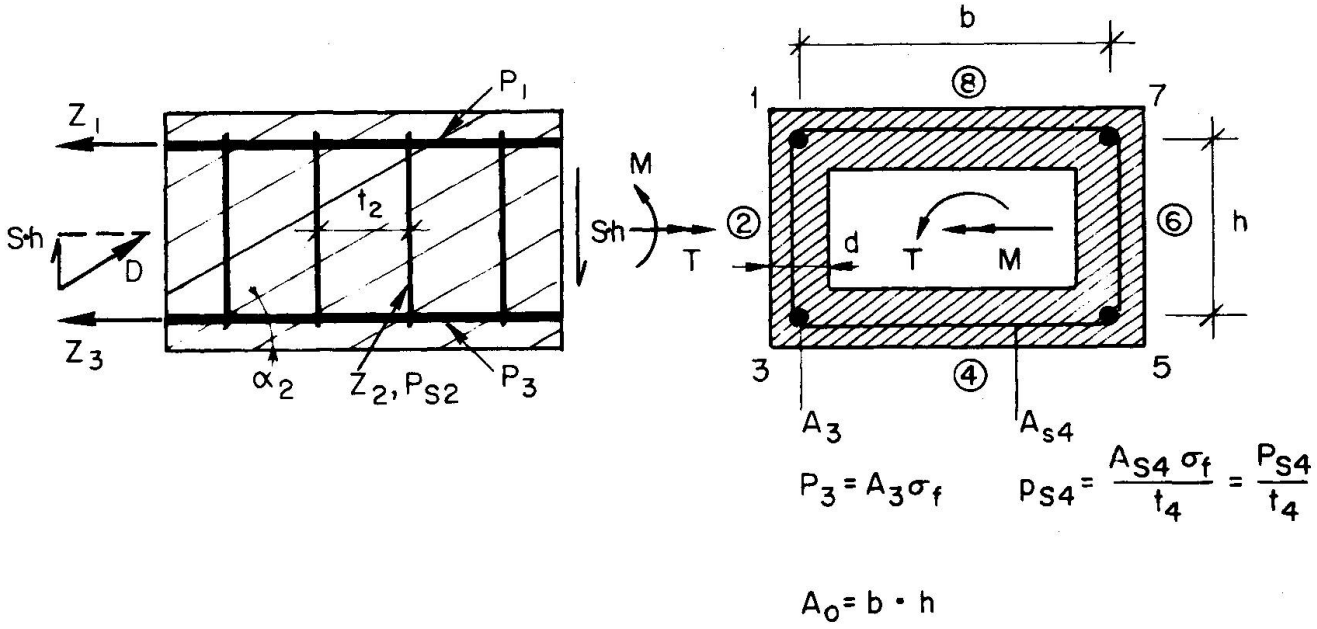

Fig. 8 Box-Section, Space Truss Model

A statical solution is given first. A space truss model is assumed with the stringers as chords, the stirrups as posts and the concrete forming diagonal compression fields under angles α [5], [6]). The walls are under pure shear such that Eqs. (2), (3), (4) and (5) are directly applicable. For wall 2 the following force system develops:

Stirrup force: $Z_2 = S \cdot t_2 \cdot \tan\alpha_2 = p_{s2} \cdot t_2$

Yielding of the stirrups, $Z_2 = p_{s2} \cdot t_2$, fixes the angle α_2:

$$\cot\alpha_2 = \frac{S}{p_{s2}} \tag{26}$$

Horizontal component D_h of compression field:

$$D_{h2} = S \cdot h \cdot \cot\alpha_2 \tag{27}$$

Failure may occur by yielding of the stirrups and the two lower stringers (Regime I). Equilibrium of the internal forces with respect to the axis 1-7 gives

$$D_{h2} \cdot \frac{h}{2} + D_{h4} \cdot h + D_{h6} \cdot \frac{h}{2} - Z_3 \cdot h - Z_5 \cdot h = 0 \tag{28}$$

Replacing Z_3 and Z_5 by the yield forces P_3 and P_5 of the stringers and making use of Eqs. (26) and (27) gives

$$S^2 = \frac{P_3 + P_5}{\frac{h}{2}\left(\frac{1}{p_{s2}} + \frac{1}{p_{s6}}\right) + b \cdot \frac{1}{p_{s4}}} \tag{29}$$

and the collapse moment T_{po}

$$T_{po} = 2A_o \sqrt{\frac{P_3 + P_5}{\frac{h}{2}\left(\frac{1}{p_{s2}} + \frac{1}{p_{s6}}\right) + b\,\frac{1}{p_{s4}}}} \tag{30}$$

For a constant stirrup reinforcement around the perimeter and equal stringers in all corners

$p_s = p_{s2} = p_{s4} = p_{s6}$; $\quad u = 2(h+b)$ (perimeter)

$P = P_1 = P_3 = P_5 = P_7$; $\quad A_o = b \cdot h$ (enclosed area)

the resulting expression is

$$T_{po} = 2A_o \sqrt{\frac{4P \cdot p_s}{u}} \tag{31}$$

The analysis has been extended to beams with polygonal cross sections and arbitrary reinforcements. Physically the compression fields in all walls take inclinations depending on the yield values p_s and the shear flow, Eq. (26). The stringers connecting the two rigid parts across the failure zone have to resist the horizontal components of the compression field in the walls. Failure occurs if all but two stringers in one wall will yield.

If in addition to torsion a bending moment is acting its influence on the stringer

forces have to be taken into account. Assuming for simplicity a section with constant reinforcements:

Upper stringers: $P_1 = P_7 = P_u \leqslant P_l$

Lower stringers: $P_3 = P_5 = P_l$

Stirrups : p_s

A part of the yield forces in the lower stringers will be used up by the bending moment

$$M_p = 2 \cdot h \cdot \eta \cdot P_l \; ; \qquad \eta \leqslant 1$$

Accordingly, the torsional moment will be reduced to

$$T_p = 2A_o \sqrt{\frac{4(1-\eta) \cdot P_l \cdot p_s}{u}}$$

Introducing the reference values

$$M_{po} = 2 \cdot h \cdot P_l$$

$$T_{po} = 2A_o \sqrt{\frac{4P_u \cdot p_s}{u}}$$

where T_{po} is governed by the smaller yield value $P_u < P_l$ (failure about axis 3-5 through lower stringers) the following interaction equations can be derived

Yielding $Z_l = P_l$:
$$\frac{P_u}{P_l}\left(\frac{T_p}{T_{po}}\right)^2 + \frac{M_p}{M_{po}} = 1 \qquad (32)$$

Yielding $Z_u = P_u$:
$$\left(\frac{T_p}{T_{po}}\right)^2 - \frac{P_l}{P_u} \cdot \frac{M_p}{M_{po}} = 1 \qquad (33)$$

Recently, the corresponding kinematic solution has been developed ([8], [9]). In Fig. 9 a kinematically admissible mechanism is presented. Starting from the fact that a crack ABC over two sides is only possible if the shape of the cross-section is distored, a second crack DEF on the two opposite sides is added in order to restore the original shape. In this way a parallelogram CBFE on side 4 is cut out. A rotation $\dot{\omega}$ around the axis AD through the crack ends becomes possible if the axis AD is parallel to the line CF, hence, $l_{AD} = l_{CF}$. For the displacement of point F will be perpendicular to the axis AD. On the other hand, F being located on the parallelogram will rotate perpendicularly to line FC, hence, FC parallel to AD. The angles of the two cracks CB and EF being identical, α_4, the angle β of the axis AD follows to

$$l_{CF} = b \cdot \cot\alpha_4 + h \cdot \cot\alpha_2 - l_{AD} + h \cdot \cot\alpha_6 + b \cdot \cot\alpha_4$$

with: $l_{CF} = l_{AD}$ and $\cot\beta = \frac{l_{AD}}{b}$

$$\cot\beta = \cot\alpha_4 + \frac{1}{2} \cdot \frac{h}{b}(\cot\alpha_2 + \cot\alpha_6) \qquad (34)$$

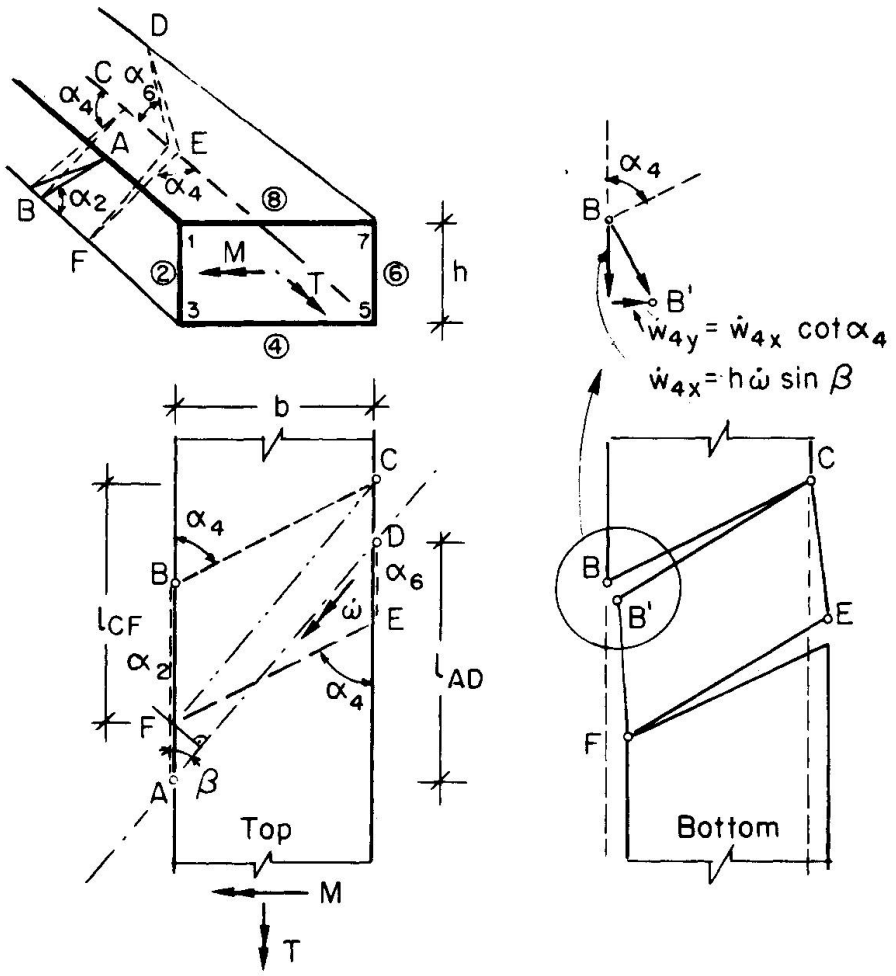

Fig. 9 Torsional Mechanism

It should be remarked that the "skew bending theory" ([10]) uses a mechanism which introduced sliding in a crack. However, the corresponding energy dissipation is erroneously neglected. Hence, the discrepancies with correct plastic solutions can be fully explained.

In order to express the energy dissipation the velocity components of point B (equal to point E) are needed (Fig. 9)

Wall 4: $\dot{w}_{4x} = \dot{\omega} \cdot h \cdot \sin\beta$, $\dot{w}_{4y} = \dot{w}_{4x} \cdot \cot\alpha_4$

Wall 2: $\dot{w}_{2x} = \dot{\omega} \cdot h \cdot \sin\beta$, $\dot{w}_{2y} = \dot{w}_{2x} \cdot \cot\alpha_2$

Using the reinforcements shown in Fig. 8 the work equation takes the form

$$L_{in} = \dot{w}_{4x}(P_3+P_5) + \frac{1}{2} \cdot p_{s2} \cdot h \cdot \dot{w}_{2x} \cdot \cot^2\alpha_2 + p_{s4} \cdot b \cdot \dot{w}_{4x} \cdot \cot^2\alpha_4 + \frac{1}{2} \cdot h \cdot \dot{w}_{6x} \cdot \cot^2\alpha_6 \cdot p_{s6}$$

$$L_{ex} = M \cdot \dot{\omega} \cdot \sin\beta + T \cdot \dot{\omega} \cdot \cos\beta$$

$$M + T \cdot \cot\beta = h(P_3+P_5) + \frac{1}{2} \cdot p_{s2} \cdot h^2 \cdot \cot^2\alpha_2 + p_{s4} \cdot b \cdot h \cdot \cot^2\alpha_4 + \frac{1}{2} \cdot p_{s6} \cdot h^2 \cdot \cot^2\alpha_6$$

Introducing $\cot\beta$ from Eq. (34) gives

$$M = h(P_3+P_5) + \frac{1}{2}(h^2 \cdot p_{s2} \cdot \cot^2\alpha_2 - \frac{h}{b} \cdot T \cdot \cot\alpha_2) + \frac{1}{2}(h^2 \cdot p_{s6} \cdot \cot^2\alpha_6 - \frac{h}{b} \cdot T \cdot \cot\alpha_6) + \frac{b}{h}(h^2 \cdot p_{s4} \cdot \cot^2\alpha_4 - \frac{h}{b} \cdot T \cdot \cot\alpha_4) \quad (35)$$

If T is fixed the minimum value of M with respect to the angles α follows from

$$\frac{\partial M}{\partial(\cot\alpha_2)} = 2 \cdot h^2 \cdot p_{s2} \cdot \cot\alpha_2 - \frac{h}{b} \cdot T = 0$$

$$\cot\alpha_2 = \frac{T}{2 \cdot b \cdot h} \cdot \frac{1}{p_{s2}} = \frac{S}{p_{s2}} \quad ; \qquad S = \frac{T}{2 \cdot b \cdot h} = \frac{T}{2A_o}$$

and similarly: $\cot\alpha_4 = \frac{S}{p_{s4}}$; $\cot\alpha_6 = \frac{S}{p_{s6}}$

Hence, the minimum M will result if T produces a constant shear flow S. This corresponds to the assumption of a constant flow in the statical solution, Eq. (25). In the case of M = 0, Eq. (35) gives the torsional moment T_{po} by introducing the values of $\cot\alpha$:

$$T_{po} = 2A_o \sqrt{\frac{P_3 + P_5}{\frac{h}{2}(\frac{1}{p_{s2}} + \frac{1}{p_{s6}}) + \frac{b}{p_{s4}}}} \quad (36)$$

With a moment M acting, Eq. (35) leads to interaction equations identical to Eqs. (32) and (33). Hence, the identity between the static and kinematic approach has been shown.

The total length of the mechanism is:

$$l_{AC} = h \cdot \cot\alpha_2 + b \cdot \cot\alpha_4 \ , \qquad \text{if } \cot\alpha_2 > \cot\alpha_6$$

or

$$l_{DF} = b \cdot \cot\alpha_4 + h \cdot \cot\alpha_6 \ , \qquad \text{if } \cot\alpha_6 > \cot\alpha_2$$

If geometrical restraints do not allow such a length warping will become necessary and a higher resistance will result. Statical solutions with a constant shear flow hence become lower bounds.

The case may also arise, where the statical solution would imply a concrete stress exceeding the strength $\sigma_c < -f_c$ in a particular wall (Regimes II or III). A redistribution of the stress field will take place leading to a non-uniform shear flow around the perimeter. A safe value is obtained if the solution with constant shear flow but $\sigma_c < -f_c$ is reduced by the factor $-f_c/\sigma_c$.

The above mentioned problems have been treated in Refs. [9] and [11]. The case of beams with open cross sections including warping has also been studied [12].

So far, only box-sections have been considered. However, in Ref. [9] it is shown that the previously discussed mechanisms are kinematically admissible also for solid cross-sections. The beam parts are separating internally in perpendicular directions. The parts are touching only along the perimeter. In reality the concrete stresses have to be transmitted over a finite wall thickness in order to

stay above the value $-f_c$. The determination of the effective wall thickness can only be made on the basis of experimental studies. In Refs. [5] and [6] such values have been proposed.

The secondary effect due to distortion of the side walls of a box section, i.e. plate bending, influences only the concrete stresses as the membrane stresses of the compression field are superimposed by secondary bending stresses ([5], [6]). Again this influence must be taken into account in a pragmatic manner by adopting a cautious value for the effective concrete strength.

4. SHEAR AND BENDING

As a statical model a truss model, Fig. 10, is used with the upper and lower stringers as chords, the stirrups as posts and the concrete as diagonal compression field under an angle α ([5], [7]):

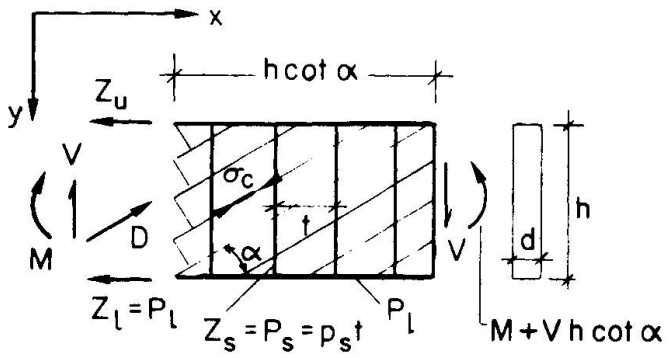

$$D = \frac{V}{\sin\alpha} \tag{37}$$

$$Z_l = \frac{M}{h} + \frac{1}{2}\cdot V\cdot\cot\alpha = P_l \tag{38}$$

$$Z_u = -\frac{M}{h} + \frac{1}{2}\cdot V\cdot\cot\alpha \tag{39}$$

$$Z_s = \frac{V\cdot t}{h}\cdot\tan\alpha = p_s\cdot t \tag{40}$$

$$\sigma_c = \frac{-D}{d\cdot h\cdot\cos\alpha} = -\frac{V}{d\cdot h}\cdot\frac{1}{\sin\alpha\cdot\cos\alpha} \tag{41}$$

Fig. 10 Truss Model Bending - Shear

The stirrup reinforcement is constant along the axis. The lower stringer reinforcement varies such that the yield value $P_l(x)$ is just reached at a critical section, hence, $Z_u = P_l(x)$. Excluding concrete failure the stirrup force Z_s will also reach the yield value $p_s\cdot t$ (Regime I). Replacing in Eq. (38) $\cot\alpha$ by its value from Eq. (40) gives the interaction equation

$$M_p + \frac{V_p^2}{2p_s} = P_l\cdot h$$

With the reference values

$$M_{po} = P_l\cdot h \quad ; \qquad V_{po} = \sqrt{2P_l\cdot p_s\cdot h}$$

$$\frac{M_p}{M_{po}} + \left(\frac{V_p}{V_{po}}\right)^2 = 1 \tag{42}$$

However, a limiting value is reached when $\sigma_c = -f_c$ (Regime II):

$$\sigma_c = -\frac{V}{d\cdot h}\cdot\frac{1}{\sin\alpha\cdot\cos\alpha} = -f_c$$

$$V_{pc} = p_{sc}\cdot h\cdot\cot\alpha$$

Hence, $$\frac{p_{sc}}{f_c\cdot d} = \sin^2\alpha$$

and

$$\frac{V_{pc}}{f_c \cdot d \cdot h} = \sqrt{\frac{p_{sc}}{f_c \cdot d}\left(1 - \frac{p_{sc}}{f_c \cdot d}\right)}$$

with the maximum value

$$\frac{\partial V_{pc}}{\partial\left(\frac{p_s}{f_c \cdot d}\right)} = 0 \quad ; \quad \frac{p_{sc}}{f_c \cdot d} = \frac{1}{2} \; ; \; \left(\frac{V_{pc}}{f_c \cdot d \cdot h}\right)_{max} = \frac{1}{2}$$

Introducing as reference value the maximum value V_{fc} governed by the concrete strength alone (Regime III):

$$V_{fc} = \frac{1}{2} \cdot f_c \cdot d \cdot h \tag{43}$$

the ratio becomes (Fig. 11(b)):

$$\frac{V_{pc}}{V_{fc}} = 2 \sqrt{\frac{p_{sc}}{f_c \cdot d}\left(1 - \frac{p_{sc}}{f_c \cdot d}\right)} \tag{44}$$

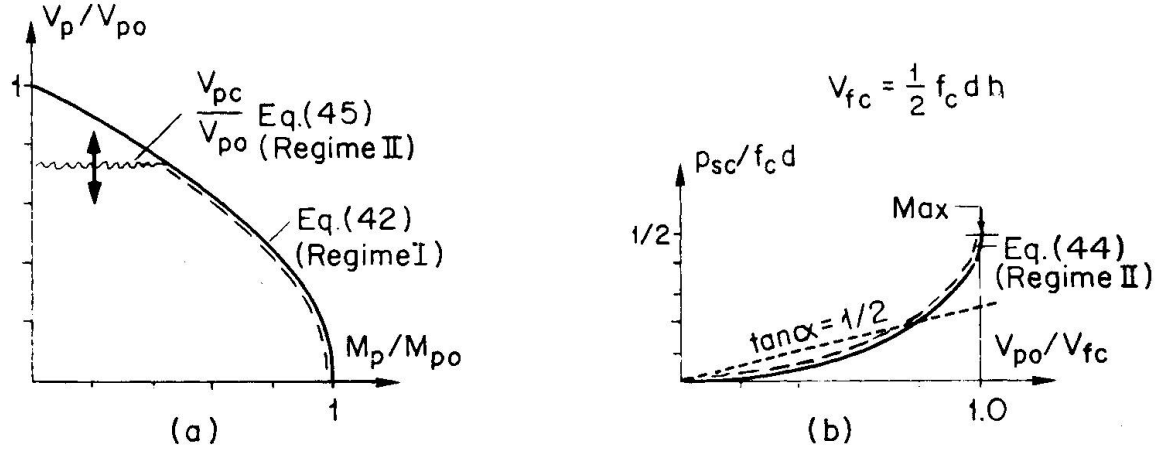

Fig. 11 Interaction Bending - Shear

The interaction Eq. (42) will be cut off if V_p reaches the value V_{pc}, hence,

$$\frac{V_{pc}}{V_{po}} = \sqrt{\frac{V_{fc}}{P_1}\left(1 - \frac{p_{sc}}{f_c \cdot d}\right)} = \sqrt{\frac{V_{fc} \cdot h}{M_{po}}\left(1 - \frac{p_{sc}}{f_c \cdot d}\right)} \tag{45}$$

These relations are shown in Fig. 11(a) and (b). Also indicated is the influence of a limitation $\tan\alpha = 1/2$ for reasons discussed previously.

Turning to the kinematic solution the mechanism is sketched in Fig. 12 ([5], [7], [13], [14]). The work equation gives:

$$M_p \cdot \dot{\omega} + V_p \cdot \dot{\omega} \cdot h \cdot \cot\alpha = P_1 \cdot \dot{\omega} \cdot h + \frac{1}{2} \cdot \dot{\omega} \cdot h \cdot \cot\alpha \cdot p_s \cdot h \cdot \cot\alpha$$

$$M_p = -V_p \cdot h \cdot \cot\alpha + \frac{1}{2} \cdot h^2 \cdot p_s \cdot \cot^2\alpha$$

with the minimum

$$\frac{\partial M_p}{\partial(\cot\alpha)} = -V_p \cdot h + h^2 \cdot p_s \cdot \cot\alpha \rightarrow \cot\alpha = \frac{V_p}{h \cdot p_s}$$

Using the previously introduced reference values M_{po} and V_{po} the interaction Eq. (42) is again obtained. Hence, the two solutions are identical.

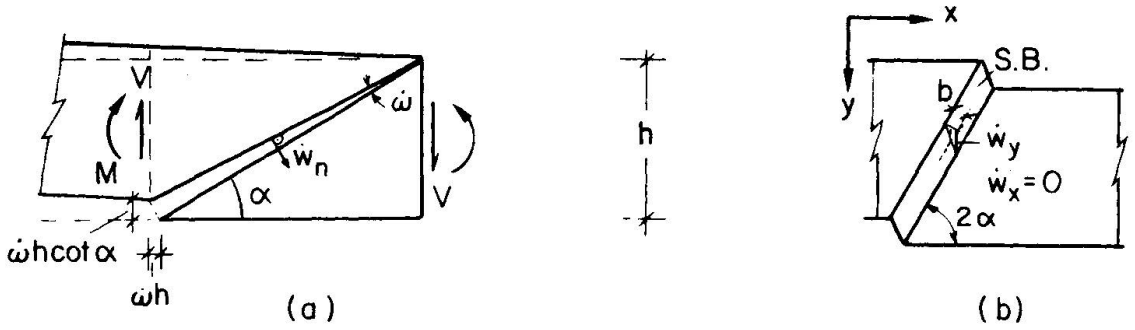

Fig. 12 Mechanism Bending - Shear

The mechanism of Fig. 12(b) corresponds to the case, where the lower stringer is not yielding but instead the concrete is failing, i.e. $\dot{\varepsilon}_2 < 0$ (Regime II). As discussed in chapter 2 a slip band (S.B.) will form at an angle 2α with α being the angle of the compression field. The collapse load will be identical to the solution, Fig. 12(a) for such a value of P_1 that $\sigma_c = -f_c$ will just be reached (transition Regime I to Regime II).

Concerning the strain ratios the same remarks hold as made under chapter 2, Eqs. (23) and (24). A small longitudinal strain $\varepsilon_{x\ tot}$ will produce very large stirrup strains $\varepsilon_{y\ tot}$ and crack strains $\varepsilon_{n\ tot}$ and a progressive break-down of the aggregate interlock for small angles α. Hence, again the necessity for a limitation of $\tan\alpha \geq 1/2$ is evident.

For a general case, where bending M, shear V and torsion T are acting on a box beam such as shown in Fig. 8, statical solutions have been presented assuming a constant shear flow for torsion superimposed by shear forces V/2 in the two side walls [5]. Interaction equations can readily be developed. Corresonding kinematic solutions have not been found. It has, however, been shown for special cases that warping effects will take place [9], [11]. Hence, the statical solution described above constitutes only a lower bound.

So far, all solutions presented have taken into account the spacial dimensions of the beams also in the transverse directions. However, beam theories for closed and open cross-sections have already been developed paralleling in concept the one-dimensional elastic beam theory ([9], [12]). Introducing as generalized stresses the resultants N, M, V and T the corresponding kinematic terms (generalized strains) in the form of extension-, curvature-, shearing- and warping-rates along the beam axis have to be properly selected. The yield criterion and the flow rules are then expressed as functions of these generalized stresses and strains. For cases when collapse is governd solely by yielding of the reinforcements (Regime I) complete beam theories have been worked out. Difficulties arise when strain rates $\dot{\varepsilon}_2 < 0$ for the case $\sigma_c = -f_c$ (point B, Fig. 2(b), (Regime II))

arise. At present, it seems improbably that for such cases a general beam theory can be developed.

5. DETAILS

Problems of structural details and some special problems are shortly indicated and appropriate references are given.

The case of concentrated loads or reactions is sketched in Fig. 13. The length $h \cdot \cot\alpha$ of the regular compression field is concentrated by a compression fan into the width e resulting into a uniform distribution of P over e. It can be easily shown by geometric relations that the concrete stress σ_c of the regular field increases at point A to σ_{cA}

$$\sigma_{cA} = \sigma_c \cdot \frac{h}{e} \cdot \cot\alpha$$

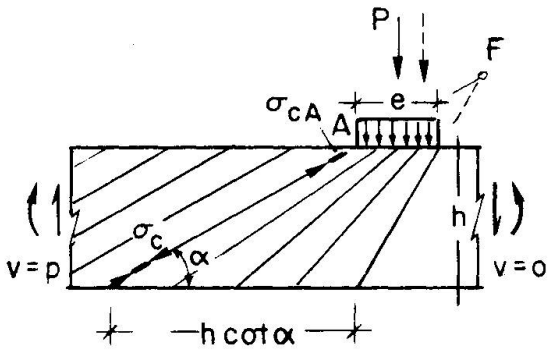

Fig. 13 Compression Fan under Concentrated Load

Hence, a relatively high stress concentration may occur. With a multi-centered fan resulting into a shift of the load P to the right and hence a non-uniform bearing stress more favourable conditions are obtained. Nevertheless, the problem of stress concentrations in such cases has to be taken into account. Further cases of end and intermediate reactions, indirect load applications through cross beams, etc. are studied in Refs [5], [9].

The proportioning of the longitudinal steel in the tension flange of a beam is essentially governed by Eq. (38). The problem of the anchorage length of bars beyond the theoretical cut off point is presented in Ref. [5].

Joints connecting beams and columns have been plastically analyzed (references mentioned in [14]). They offer special problems as transverse splitting of the elements is a distinct failure possibility.

In Ref. [9] the influences of a variable beam depth, of distributed loads and single concentrated loads are studied and the consequences for the detailing of the stirrup and longitudinal reinforcement are stated.

The membrane stress state produced by shear in a shear web can be disturbed by transverse bending moments. A box girder bridge presents such a case, where the side walls are subjected to shear in longitudinal direction and transverse bending moments resulting from transverse bending of the road slab. A static solution [15] and a complete solution [16] have been developed for this case.

6. THEORY, EXPERIMENTAL VERIFICATION, APPLICATION

Plastic solutions for the strength of beams with general cross sectional shapes subjected to bending, shear, torsion and combined actions have been developed. For many cases the correct solutions are known (i.e. static equal to kinematic solution). For other cases lower (static) and/or upper (kinematic) bounds are available.

The necessary structural details (stirrup spacing, stringer arrangement, concentrated loads, bar cut-off, etc.) have or can be developed especially from the statical solutions, where the admissible stress fields furnish the required information.

All these solutions are correct within the assumptions of the theory of plasticity, essentially

1. Rigid-ideally plastic material behaviour
2. Yield criteria and associated flow rules.

Hence, experimental verifications should essentially concentrate on checks of these assumptions and possible adjustments.

Concerning the reinforcing steels they exhibit generally plastic deformations under the yield stress which are a multiple of the elastic deformations such that the latter can be neglected. On the contrary the strength of concrete is definitely affected by deformations and/or cracks preceding failure. A considerable redistribution of the concrete stresses from initial cracking up to collapse (i.e. variation of $\alpha = \pi/4$ to $\alpha \to 0$ or $\alpha \to \pi/2$ of the compression field) accompanied by considerable cracking will markedly diminish the strength. The redistribution may further be limited by the progressive deterioration of the aggregate interlock in previously formed cracks such that the orthogonality required by the flow rules may no longer hold.

The assessment of the effective concrete dimensions offers another problem. Under conditions, where the concrete strength is governing and large redistributions occur the concrete cover may spall off prior to failure. In other instances when failure due to yielding of the reinforcement occurs at low concrete stresses the cover will stay intact.

Only results from experiments on properly detailed specimens (see chapter 5) tested under clearly definited conditions (e.g. necessary extent of mechanism, chapter 3) should be compared with the corresponding theoretical values. It is evident that tests with premature failures of details and/or unclear testing conditions must be excluded.

Considerable experimental evidence has already been collected supporting the applicability of plastic analysis to determine the ultimate strength of reinforced concrete beams. A proper and cautious selection of the effective concrete strength f_c must be made reflecting the above mentioned influences. The fixing of the effective concrete dimensions becomes important if failure is governed by the concrete strength and large redistributions.

It is felt that plastic analysis offers a rational, unified, simple, economical, safe and reasonably accurate method to calculate the static strength of reinforced concrete beams (and slabs and walls as well). It will become more generally applied as the concept of limit state design is gaining general acceptance. For in this concept one of the limit states to consider is the ultimate limit state.

So far design rules for beams under bending, shear, torsion and combined actions based on plastic analysis have already been introduced in the Swiss specifications [19] and the new CEB Model-Code (Shear, Torsion, refined method) ([17], [18], [20]).

References

1 Nielsen, M.P.: "Yield Conditions for Reinforced Concrete Shells in the Membrane State", Reprint from Non-Classical Shell Problems, Proc. IASS Symposium Warsaw, Sept. 2.-5. 1963.

2 Nielsen, M.P.: "On the Strength of Reinforced Concrete Discs", Acta Polytechnica Scandinavica, Copenhagen, 1971, p. 261.

3 Jensen, B.C.: "Lines of Discontinuity for Displacements in the Theory of Plasticity of Plain and Reinforced Concrete", Magazine of Concrete Research, Vol. 27, No. 92, 1975, p. 143.

4 Marti, P., Thürlimann, B.: "Fliessbedingung für Stahlbeton mit Berücksichtigung der Betonzugfestigkeit" (Yield Criteria for Reinforced Concrete Including the Tensile Strength of Concrete), Beton- und Stahlbetonbau, Heft 1, 1977.

5 Thürlimann, B., Grob, J., Lüchinger, P.: "Torsion, Biegung und Schub in Stahlbetonträgern" (Torsion, Bending and Shear in Reinforced Concrete Beams), Institut für Baustatik und Konstruktion, ETH Zürich, Autographie zu Fortbildungskurs für Bauingenieure aus der Praxis, 1975.

6 Lampert, P., Thürlimann, B.: "Ultimate Strength and Design of Reinforced Concrete Beams in Torsion and Bending", Publications, International Association for Bridge and Structural Engineering (IABSE), Vol. 31-I, p. 107, 1971.

7 Grob, J., Thürlimann, B.: "Ultimate Strength and Design of Reinforced Concrete Beams under Bending and Shear", Publications, International Association for Bridge and Structural Engineering (IABSE), Vol. 36-II, p. 105, 1976.

8 Müller, P.: "Failure Mechanisms for Reinforced Concrete Beams in Torsion and Bending", Publications, International Association for Bridge and Structural Engineering (IABSE), Vol. 36-II, p. 147, 1976.

9 Müller, P.: "Plastische Berechnung von Stahlbetonscheiben und -balken" (Plastic Analysis of Walls and Beams of Reinforced Concrete), Institut für Baustatik und Konstruktion, ETH Zürich, Bericht Nr. 83, Birkhäuser Verlag Basel und Stuttgart, 1978.

10 Gvozdev,A.A., Lessig, N.N., Rulle, L.K.: "Research on Reinforced Concrete Beams Under Combined Bending and Torsion in the Soviet Union"; Torsion of Structural Concrete, Journal American Concrete Institute, April 1968, p. 310, Publication SP-18.

11 Lüchinger, P.: "Bruchwiderstand von Kastenträgern aus Stahlbeton unter Torsion, Biegung und Querkraft" (Ultimate Strength of Box-Girders in Reinforced Concrete under Torsion, Bending and Shear), Institut für Baustatik und Konstruktion, ETH Zürich, Bericht Nr. 69, Birkhäuser Verlag Basel und Stuttgart, 1977.

12 Grob, J.: "Traglast von Stäben mit dünnwandigen offenen Querschnitten" (Ultimate Strength of Beams with Thin-Walled Open Cross-Sections), Institut für Baustatik und Konstruktion, ETH Zürich, Bericht Nr. 56, Birkhäuser Verlag Basel und Stuttgart, 1975.

13 Braestrup, M.W.: "Plastic Analysis of Shear in Reinforced Concrete", Magazine of Concrete Research, Vol. 26, No. 89, December 1974.

14 Nielsen, M.P., Braestrup, M.W., Bach, F.: "Rational Analysis of Shear in Reinforced Concrete Beams", Proceedings, IABSE, P-15/78, May 1978.

15 Thürlimann, B.: " Schubbemessung bei Querbiegung" (Shear Design considering Cross Bending), Schweiz. Bauzeitung, Heft 26, p. 478, 1977.

16 Marti, P., Thürlimann, B.: "Shear Strength of Reinforced Concrete Walls with Transverse Bending", (in preparation).

17 Thürlimann, B.: "Shear Strength of Reinforced and Prestressed Concrete Beams - CEB Approach", ACI-Symposium 1976, Philadelphia, (Proceedings in preparation).

18 Thürlimann, B.: "Torsional Strength of Reinforced and Prestressed Concrete Beams - CEB Approach", ACI-Symposium 1976, Philadelphia (Proceedings in preparation).

19 Richtlinie 34 zu Norm SIA 162, 'Bruchwiderstand und Bemessung von Stahlbeton- und Spannbetontragwerken' (Directive RL 34 to Structural Design Code SIA 162 (1968)), Schweizerischer Ingenieur- und Architekten-Verein, Zürich, 1976.

20 Comité Euro-International du Béton: "Code modèle pour les structures en béton", Système international de règlementation technique unifiée des structures, vol. II, Bulletin d'Information, No. 117, Paris, décembre 1976.